THE UNIVERSITY OF MANITOBA

INTERACTIONS OF SMALL MOLECULES WITH BIOPOLYMERS AS STUDIED BY PULSE RADIOLYSIS

by

S.D. Banerjee

A THESIS

Submitted to the Faculty of Graduate Studies in partial fulfillment of the requirements for the degree of Master of Science.

Department of Physics

Winnipeg, Manitoba

1980

INTERACTIONS OF SMALL MOLECULES WITH BIOPOLYMERS AS STUDIED BY PULSE RADIOLYSIS

BY

SANDHYA DENISE BANERJEE

A thesis submitted to the Faculty of Graduate Studies of the University of Manitoba in partial fulfillment of the requirements of the degree of

MASTER OF SCIENCE

ACKNOWLEDGEMENTS

I wish to extend my sincere appreciation to Dr. C.L. Greenstock for his guidance, patience and encouragement during the course of this research and the writing of this thesis.

I also wish to thank Dr. A. Petkau for his supervision and many helpful suggestions.

This research was conducted at the Whiteshell Nuclear Research Establishment in Pinawa, Manitoba. I am grateful to Atomic Energy of Canada Ltd. for allowing me the use of their facilities.

TABLE OF CONTENTS

ABSTRACT

Molecular interactions may cause a wide variety of effects including modification of radiation sensitivity, mutagenesis, carcinogenesis, antibiotic and antitumour activity. The quantitative aspects of the interactions of small molecules with biopolymers have been investigated by the Pulse Radiolysis technique. Binding parameters calculated with this technique for the interaction of mutagenic acridine dyes with nucleic acids agree with results obtained by conventional techniques. The interactions of the toxic herbicide paraquat and radiation modifiers with DNA have been investigated. The method has also been used to determine the effect of macromolecular conformation on molecular association, and the aggregation of both small molecules and macromolecules.

When molecules associate they form bulky complexes with low diffusion coefficients. The apparent rate of reaction of the primary reactive species e^-_{aq} (hydrated electron), formed in the radiolysis of water, depends mainly on the diffusion coefficients and encounter radii of the reactants. The reactivity of e^-_{aq} is greater with freely diffusing molecules than with molecular complexes. Changes in ionic strength, molecular conformation or aggregation result in changes in e^-_{aq} reactivity, which is used as a measure of complex formation.

The reactive species e^-_{aq} was generated by nanosecond pulses of 3 MeV electrons from a Van de Graaff accelerator. Changes in e^-_{aq} reactivity were measured by monitoring changes in e^-_{aq} absorption at 650 nm by kinetic spectrophotometry.

The Pulse Radiolysis technique is simple, swift and accurate, and provides a powerful method based on chemical kinetics to study molecular interactions. It is an *in situ* method, which does not disturb the equilibrium of any interaction under study, nor require a separative or analytical measure of binding. It has potential in investigating radiation damage to, and the effects of radiation modifiers on, cell components in simple model systems.

Page

Chapter 1

INTRODUCTION

It is important to understand the mechanisms and the consequences of molecular interactions because these interactions, leading to the formation of molecular complexes, are encountered in countless and diverse biochemical systems. Many of these interactions are essential to life, such as the combination of oxygen and hemoglobin, or complex formation between enzymes, substrates and coenzymes. The action of many drugs, antibiotics and antitumour agents is due to complex formation with DNA or other biological macromolecules (1,2,3,4). Aminoacridines such as acridine orange and proflavine are known to inhibit nucleic acid synthesis (5). Many mutagens and carcinogens are known to associate with key biological macromolecules such as nucleic acids and proteins (6). The chemical action of radiosensitizers and radioprotectors may be due, in part, to their association with key target macromolecules (7,8). The mechanism of these interactions and the factors that affect them are, therefore, of great importance.

a) Introduction to the Pulse Radiolysis Technique

In the course of the investigation of the reactions of free radicals with nucleic acids, it was found that the reactivity of primary free radical species, particularly the hydrated electron, e^-_{aq}, with nucleotides, dropped two orders of magnitude when these same nucleotides were incorporated into DNA (9). Free radical reactivity was greater with small, freely diffusing solute subunit molecules, than with large bulky macromolecules incorporating these subunits such

as DNA. This is to be expected, because the absolute rate constants for the reactions of e^-_{aq} with solute molecules are determined by the diffusion coefficients and encounter radii of the reactants (10).

This observation opened up a whole new area of application of the pulse radiolysis method. The change in e^-_{aq} reactivity could be qualitatively and quantitatively related to the assembly of small molecules into macromolecules. If the mobility of a reactant is reduced either by association with a less mobile large molecule, or by self association, its diffusion controlled reactivity with e^-_{aq} will be reduced. Conformational changes in macromolecules may aid association and change diffusibility.

For well over a decade, the pulse radiolysis method (11) has been used to study the reactions of transient free radical species, generated in dilute solutions by a short intense burst of ionizing radiation, with solute molecules (12). Biologically important molecules may interact directly with incident radiation (direct action) or with radical species produced by the action of ionizing radiation on solvent molecules (indirect action). In dilute aqueous solutions the latter process predominates. The cellular environment is approximately 70% water and so indirect action will predominate. The indirect action of radiation has therefore been the subject of extensive research.

In irradiated aqueous solutions, the primary reactive species are the hydrated electron and the hydroxyl free radical (e^-_{aq} and .OH). They are both highly reactive and can be detected by kinetic spectrophotometry. Their reaction rate constants, ($\leq 10^{10}$ M^{-1} s^{-1}), are

listed in Table 1 for various cell components.

In order to simplify the study of the reactions of either e^-_{aq} or .OH, the interfering radical is removed by the addition of a suitable scavenger to the solution. Oxygen scavenges e^-_{aq}, and t-butanol is a good .OH scavenger. Under appropriate scavenging conditions, the reaction of a single remaining free radical with a particular biological molecule such as DNA, resulting in a change in chemistry of the molecule, may be followed.

The e^-_{aq} was chosen as the primary reactive species and .OH scavenged with t-butanol because e^-_{aq} has an intense broad absorption band peaking at 720 nm (13), enabling its reactions to be easily monitored. Pulse radiolysis could then be used to study molecular interactions.

Many workers (14, 15) have utilised the fact that on binding smaller molecules, often sites on macromolecules that are reactive towards e^-_{aq} may be shielded, resulting in a decrease in e^-_{aq} reactivity. Among the interactions studied are the binding of drugs (16, 17), phospholipids (18) and ethidium bromide (19) to proteins. In order to test the validity of the idea that molecular association leading to lower diffusibility and reactivity with e^-_{aq}, could be used as a probe in binding studies, the interaction of ethidium bromide (EB) with DNA was investigated (15, 20) in this laboratory.

EB is a phenanthridine drug used in the treatment of bovine African Trypanosomiasis. Its biological action is believed to be a result of complex formation with DNA. This interaction has been investigated in detail by conventional techniques (21, 22), such as spectrophotometry, fluorometry and equilibrium dialysis. The strength and probable mechanism of the interaction are known. This was therefore

Table 1

Reaction Rate Constants for the Solvated Electron with Various Cell Components

e^-_{aq} Rate Constants ($M^{-1}s^{-1}$)	Cell Constituents
$> 10^{11}$	DNA, RNA, enzymes
$\sim 10^{10}$	Nucleic acid bases, Coenzymes, Vitamins, Nucleotides Nucleosides
$\sim 10^{9}$	Aromatic amino acids
$\leq 10^{7}$	Phosphate esters, organic acids, sugars, carbohydrates

chosen as a suitable interaction with which to check the feasibility of the pulse radiolysis method.

It was found that in the absence of DNA, the e^-_{aq} rate of decay was first order in EB concentration over a 10 fold concentration range. (Solutions were at neutral pH and .OH was scavenged by 0.1 M t-butanol). The rate constant for the reaction of e^-_{aq} with EB, $\sim 4 \times 10^{10}$ M^{-1} s^{-1}, was diffusion controlled. On the addition of DNA, the e^-_{aq} decay rate dropped dramatically, indicating a decrease in the number of small molecules free to react with e^-_{aq}. Various other small molecules, dyes and inorganic cations were tested with DNA (20). Some were known to bind DNA. Data in all cases corroborated results found by conventional methods.

A comparison of the pulse radiolysis method with conventional methods used to study molecular interactions is given in the next section.

b) Comparison of the Pulse Radiolysis Technique with Conventional Techniques

Numerous methods have been used to study the nature and mechanisms of molecular complex formation, depending upon the properties of the molecules involved. A change in optical properties on molecular association is the basis of spectrophotometric and fluorimetric methods. Optical methods can be used when the molecules involved have characteristic spectral properties (23). The binding of EB to DNA and RNA causes a shift in the visible region of the spectrum, the maximum absorption peak of the dye shifting from 479 nm to 518 nm. There is a colour change from yellow-orange to pink (21). The decrease in absorption with varying concentration of small molecules is related to the ratio

of bound molecules to nucleotides present. The absorption peak also changes with the salt concentration. A Scatchard plot (24) can be drawn with these data to determine the strength of the interaction (association constant, K, M^{-1}), and number (n) and type of binding sites per macromolecule. Fluorescent characteristics of the EB spectrum also change depending upon whether the dye interacts with free RNA, ribosomal RNA, or RNA associated with the cell membrane (25).

The binding of acridine orange and 9-aminoacridine to polyadenylic acid (poly A) and DNA has been studied optically (26) by absorption and fluorescence spectroscopy, circular dichroism (CD) and optical rotatory dispersion (ORD). Even though these methods are fairly rapid and do not involve complicated sample preparation, CD and ORD spectra are sometimes difficult to interpret due to the overlapping of electronic transitions. The crucial factor in using optical methods is that the compounds must exhibit particular optical properties in terms of being coloured or highly fluorescent.

Stopped-flow techniques are also used extensively (27). These methods can involve considerable shearing and destruction of the macromolecule involved. In the case of a biopolymer with repeating subunits such as DNA, the molecular weight may be considerably reduced. A correction would have to be made for this. The method is not very sensitive, however.

Conformational changes in polynucleotides due to the presence of divalent metal ions have been measured by studying changes in the optical rotatory dispersion (ORD) and ultraviolet spectra (28). The

conformational change may be either stabilization of helical structure or destabilization to form random coils. In either case there is a change in ORD or UV spectra that can be quantified with the degree of conformational change (28).

Equilibrium dialysis is another method used extensively. The solution under investigation is separated into a high and low molecular weight component by a semipermeable membrane that allows the passage of one type of molecule and not the other. The interaction of numerous antibiotics and DNA have been examined by this method (29). It is a slow process, however, and the time taken to reach equilibrium may be 60 to 72 hours. If one molecule is charged, the distribution of diffusible ions both inside and outside the membrane will be affected. Addition of a suitable salt may correct this problem, but the salt may also compete for binding sites on the macromolecule. This problem arises with serum albumin, as it will bind the anion of any neutral salt to some extent.

Ultrafiltration also utilizes a semipermeable membrane that selectively, in terms of molecular weight, allows the passage of molecules through it (30). Solutions are forced under pressure through the membrane. This may shear large molecules or destroy a weakly bound complex.

A shift in buoyant density has been used to study the intercalation of various molecules into closed circular DNA (31). This is a useful method if a marked change in buoyant density occurs and reveals the structure of this type of DNA molecule.

Ultracentrifugation is also used but here too there is a danger of destroying a weakly bound complex (32).

One of the most powerful analytical techniques for studying the detailed architectural structure of molecules, high resolution nuclear magnetic resonance, has been used to investigate the nature of molecular interactions. This method provides detailed information on the positions of certain nuclei within molecular structures. Changes in the chemical environment due to changes in pH, temperature, ionic strength or the addition of small molecules can be detected. The highly specific, detailed information available by this method is in marked contrast to the more general, but equally essential, information obtained by pulse radiolysis and the steady-state techniques which monitor the consequences of binding such as changes in optical absorption, fluorescence, CD, ORD, sedimentation velocity, chemical reactivity, etc.

Most nuclei have spin and charge. The possible orientations of nuclear spin give rise to different energies in an external magnetic field. If the external field has an oscillating component, energy is absorbed or emitted as the nuclear spin changes direction. This is known as nuclear magnetic resonance. In order to get the nuclear magnetic moments to line up with an external magnetic field (H_0), another rotating field (H_1) must be applied, perpendicular to H_0. These nuclei do not behave like macroscopic bar magnets. Their spin axes precess about H_0. When H_1 rotates at the precession frequency, resonance occurs and the nuclear magnetic dipoles flip over. When this occurs voltage is induced in a coil. This voltage is amplified and displayed on an oscilloscope screen (33,34,35).

Nuclei have characteristic resonant frequencies. The NMR spectra of organic molecules are complex. The resonant peaks must be resolved and assigned to specific nuclei. Fortunately, only about half

of all known isotopes have magnetic moments. If both mass and atomic number of a particular atom are even, then I = 0, where I is the spin angular momentum quantum number, and since the magnetic moment $\mu = g_N \beta_N \sqrt{I(I+1)}$ where g_N is the nuclear g factor, a dimensionless constant, and $\beta_N = \frac{e\hbar}{2Mc}$, the nuclear magneton, $\therefore \mu = 0$.

These isotopes include ^{12}C, ^{16}O and ^{32}S, so the spectra of organic molecules is somewhat simplified.

Molecular structural information may be measured by small but measurable shifts in resonant peaks of nuclei due to the chemical environment. These chemical shifts are due to the shielding effects of electron clouds around nuclei, or the proximity of protons to electronegative groups. Chemical shifts may also be caused by the presence of paramagnetic metals. Paramagnetic organic free radicals (spin-labels) that covalently attach themselves to macromolecules are used as probes. Ring currents, or currents arising from the circulation of delocalized π-electrons, produce a local magnetic field that opposes the external applied field above and below the plane of the aromatic ring. Nuclei outside the ring in the plane of the aromatic ring have their resonances shifted to low field. Nuclei inside the ring are partially shielded and higher external fields are required to achieve resonance.

These chemical shifts therefore offer detailed information on the structure of the aggregates of acridine orange molecules in solution (36) and on the interaction of nucleic acids and drugs (37 - 41).

The sensitivity of the nuclear magnetic resonance technique is determined primarily by the line width of the resonances, the natural abundance of the isotope and its NMR sensitivity. A number of overlapping peaks in the spectrum can render it extremely difficult to interpret. From a practical point of view, high resolution NMR is not a simple or convenient technique for characterizing the qualitative and quantitative aspects of binding involving large, complex molecules.

The pulse radiolysis method on the other hand yields information on a "macroscopic" level, which is an indirect result of binding, rather than a direct measure. It can be used to determine the degree of complex formation, of conformational change, aggregation, and the number and strength of binding sites on a macromolecule. Details of the conformational change at a particular site may be obtained by NMR. Even though the pulse radiolysis method utilises chemical kinetics in the analysis of binding phenomena, it is, like the other methods mentioned, a static method. The dynamics of binding are not investigated. Pulse radiolysis is an experimental technique which probes molecular interactions indirectly, by observing changes in chemical reactivity resulting as a direct consequence of the binding process which has taken place. Nature of the binding can only be inferred indirectly, by experimental observations of changes caused by external perturbation (e.g. pH, temperature, ionic strength etc.) For instance, intercalative binding can be inferred from the experimental result showing a decrease in association of acridine orange with DNA following heat denaturation of the macromolecule. Although, like many other techniques for studying binding, the pulse radiolysis method is indirect, it is, because of

the complexity of binding processes involving biopolymers, a practical and useful alternative to the highly sensitive but necessarily limited specific analytical techniques such as NMR. This is especially evident when results are needed in a short period of time and for a wide range of compounds, or for different types of binding, such as in drug screening.

No single method of investigation is universally applicable. Many methods employ optical techniques and these are necessarily limited to the study of molecules with specific optical properties, and the changes in these properties on association must be observable. Other methods are lengthy (equilibrium dialysis), involve possible shearing or destruction of molecules and complexes (stopped flow, ultracentrifugation) or time consuming sample preparation. Results of filtration experiments are confused when either molecule is charged. It is difficult to use one method to study several aspects of binding such as competitive binding and conformational changes in molecules.

The pulse radiolysis technique does not involve complicated sample preparation, simply solution preparation and dilution. Molecules are not required to have any special properties such as fluorescence, or bright colour, or exhibit changes in any properties on association. The time involved in the experiments is relatively short and data may be obtained quickly. Drugs may be rapidly screened as to their possible interaction with biologically important macromolecules. Charged molecules may be investigated, and separation of molecules is not necessary. Very small quantities of solute are required, a great advantage when using expensive substances.

In pulse radiolysis, binding is studied in situ, and may be observed under physiological conditions, without interference or perturbation of the system, allowing the possibility of investigating even delicate unstable or weak interactions. Pulse radiolysis does not measure directly the nature or mechanism of binding, but rather the physical/chemical consequences of binding which result in the formation of less mobile complexes whose chemical reactivity and diffusion reflect their altered structural properties. These consequences or results of binding are universally amenable to qualitative and quantitative analysis of binding and the static parameters involved. A lot can be inferred or deduced about the nature and mechanism of the dynamic processes involved by analysing these parameters, and the influence of environmental factors (pH etc.) on them.

Samples do have to be properly deoxygenated, to less than 10^{-6} M of oxygen, and should preferably be soluble in water. However, alcohol and other polar solvents should also be suitable. The method appears to have wide scope. Binding interactions may be studied quantitatively to determine the strength of the association and number of binding sites (15). Conformational changes may be detected by this system, whether that change be due to chemical action or physical effects such as those of ionizing radiation. A conformational change is reflected in a change in binding affinity for a particular ligand. Molecular associations can also be studied, since the diffusion coefficient of molecular aggregates is considerably less than that of individual small molecules.

c) Objectives of This Study

The objectives of this experimental study are to test the validity of the pulse radiolysis method for studying molecular associations, to evaluate it in relation to other methods used, and to explore some of the alternate ways in which this versatile method may be used. In order to accomplish this, the interaction of acridine orange and DNA was first investigated in detail.

The interactions of the aminoacridines and their derivatives with biological macromolecules have been intensively investigated because of their antibacterial, mutagenic and carcinogenic action (42). Their association with DNA results in a change in shape of the macromolecule (43). These interactions along with the interactions of other dyes such as EB, are representative of a whole class of interactions of small molecules with biological macromolecules. These substances are coloured or fluorescent and their interactions are normally observable as changes in their optical spectra. The pulse radiolysis technique was employed to study these well characterised systems, not by the change in optical properties of the ligands but by using chemical kinetics.

Since the primary interaction of EB and DNA is dependent upon the secondary structure of DNA, a change in secondary structure should be indicated by a change in primary strong binding affinity. The interaction of heat denatured DNA, polyguanylic acid (poly G) and

polyuridylic acid (poly U) were studied to verify the requirement of secondary helical structure for observing primary strong binding, and to compare these results with data from techniques utilising the change in optical properties of EB. Optimum conditions for the interaction of small molecules with DNA may thus be determined. These optimum conditions, together with the molecular characteristics of known chemical radiation modifiers, could be used to design model compounds with specific biological action. The binding affinity of the radiation modifiers cysteamine, dehydroascorbate and N-ethylmaleimide for DNA was measured. The effect of drug binding on radiation modification of the target molecule could then be evaluated.

This method has potential in the rapid screening of drugs for their possible interactions with key biological macromolecules. The structure of the herbicide paraquat suggests that it might intercalate in the DNA helix. The binding affinity of this herbicide with DNA was determined.

It should be possible to investigate the association of macromolecules by the pulse radiolysis method. Since histones have a great affinity for DNA, this association was investigated. The assocation of the small molecules 5'-guanosine monophosphate (5'GMP) and 5'-cytosine monophosphate (5'CMP) was also studied. Results obtained by high resolution NMR spectroscopy on this association and the structure of polynucleotides have been discussed, and the type of information obtained by NMR and pulse radiolysis compared.

d) Thesis Format

The format of this thesis is as follows. Chapter II contains background information: a brief review of radiation chemistry, the pulse radiolysis technique and chemical reaction kinetics. The fourth section covers the theory and mathematics used in obtaining expressions for binding parameters. Chapter III contains a brief description of the Van de Graaff accelerator, optical detection equipment and sample preparation. Experimental results are discussed in chapter IV. These results are summarised in chapter V, in relation to the objectives set out in the Introduction.

Chapter II

BACKGROUND INFORMATION

a) Radiation Chemistry of Water

When ionizing radiation penetrates and is absorbed in water, energy is transferred from the radiation beam to the water molecules, resulting in excitation and ionization of the water molecules (44). Along the path of the incident particle, excited water molecules H_2O^*, are formed, that lose their energy by non-radiative processes in $\sim 10^{-13}$ seconds.

Direct ionization also takes place along the primary particle tracks yielding ionized water molecules.

$$H_2O \longrightarrow H_2O^+ + e_s^- \qquad (1)$$

Both H_2O^+ and the electrons produced (e_s^-) interact with water molecules resulting in the production of the species H., .OH, H_2 and H_2O_2 (44, 45).

The energy of e_s^- is dissipated by ionization and dissociation of water molecules. When the energy falls below a threshold value* the electron becomes thermalized. It then reorients the dipolar water molecules to form a cage around itself, and is said to be hydrated or solvated, e_{aq}^- (45). This process occurs in $\sim 10^{-11}$ seconds.

The G-values (number of species formed per 100 eV of energy absorbed by the solution) for the yields of molecules and radicals (46) are given below:

*1.5 - 2.0eV (46)

Species formed	G-values
e^-_{aq}	2.8
.OH	2.8
H.	0.5
H_2	0.5
H_2O_2	0.8

The primary radical products of irradiated water are e^-_{aq} and .OH.

b) The Pulse Radiolysis Technique

The pulse radiolysis technique has been developed over the past twenty years (12). The method involves the formation of free radicals, ions and excited states in dilute organic or inorganic solutions, by the absorption of a well-defined short burst of ionizing radiation. The change in the optical absorption of the solution is then monitored by kinetic spectrophotometry (11). It is now possible, with the advent of high energy accelerators, to obtain pulses of nanosecond duration, and to use fast sensitive detectors to observe transient absorptions in the near U-V region of the spectrum (47).

On irradiating a dilute aqueous solution with a short pulse of ionizing radiation, the principal primary species produced are e^-_{aq} and .OH, as outlined in the previous section. One of the species is often removed by the addition of a suitable scavenger, and the absorption of the remaining radical is monitored.

In this study, 50 ns pulses of 3 MeV electrons were generated by the Van de Graaff accelerator. The absorption of e^-_{aq} at 650 nm was observed. The e^-_{aq} has a broad visible absorption band at 650 nm. In

order to demonstrate visually on an oscilloscope the formation and decay of e^-_{aq}, concentrations of at least 10^{-9} M are required, and preferably concentrations up to 10^{-7} M. This steady state concentration cannot, practically, be attained with available continuous sources of radiation because of the transient nature of e^-_{aq} (13). It can only be generated momentarily by a short pulse of radiation such as high energy electrons from an accelerator.

The .OH radicals are scavenged by the addition of t-butanol to the solutions. The resulting tertiobutyl radical is unreactive and does not absorb appreciably above 280 nm (48). The e^-_{aq} diffuses through the solution, reacting with solute molecules that it may encounter. An analysing light is passed through the solution and oscilloscope traces show the exponential decay of e^-_{aq} optical absorption at 650 nm with time. The absorbance is directly proportional to the amount of e^-_{aq} present. The rate of e^-_{aq} decay is dependent upon the solute molecules present. First-order reaction rates and rate constants may be calculated from these traces. The chemical kinetics of these reactions are described in the next section.

c) Reaction Kinetics

The rate of reaction k_D of the free radicals e^-_{aq}, .H and .OH in aqueous solutions with solute molecules depends upon the temperature, solvent dielectric constant, charges, encounter radii and diffusion constants of the reactive species and solute. According to diffusion theory (10), when either solute or reactive species is uncharged, the diffusion limited rate is,

$$k_D = 4\pi (r_1+r_2)(D_1+D_2)N.10^{-3} \quad M^{-1}s^{-1} \qquad (2)$$

where r_1 and r_2 (Å) are the encounter radii of reactive species and solute, respectively, and D_1 and D_2 (cm^2s^{-1}) are the respective diffusion constants. If the reactants are charged, a correction term must be applied to account for electrostatic effects of the charged reactants. The rate then becomes

$$k_D = 4\pi(r_1+r_2)(D_1+D_2)N.10^{-3}\{[Q_1Q_2e^2/\varepsilon KT(r_1+r_2)]/(\exp[Q_1Q_2e^2/\varepsilon KT(r_1+r_2)]-1)\} \; M^{-1}s^{-1} \qquad (3)$$

where Q_1 and Q_2 (esu) are the charges on the reactive species and solute respectively, ε is the solvent dielectric constant, and T is the temperature (^oK).

For e^-_{aq}, $D_1 = 4.5 \times 10^{-5}$ $cm^2 .s^{-1}$ and $r_1 = 3\text{Å}$ (13). The calculated rate constants for diffusion controlled reactions with most small molecules are of the order of $2\text{-}4 \times 10^{10} M^{-1}s^{-1}$.

The reaction of the absorbing species e^-_{aq} and solute molecules (represented by "S") is of the form

$$e^-_{aq} + S \xrightarrow{k_s^1} \text{Product} \qquad (4)$$

At low doses the observed rate of decay of e^-_{aq} (k'obs) is constant and the reactions are pseudo first-order. The disappearance of e^-_{aq} may be represented by the following equation:

$$\frac{d[e^-_{aq}]}{dt} = - k'_{obs} [e^-_{aq}] \qquad (5)$$

The solution to equation (5) is

$$[e^-_{aq}]_t = [e^-_{aq}]_o \, e^{-k'_{obs}t} \qquad (6)$$

where $[e^-_{aq}]_o$ is the initial e^-_{aq} concentration.

Since the absorbance of the solution through which the analysing light passes is directly proportional to the concentration of e^-_{aq}, the concentrations may be replaced by absorbance (A). Equation (6) may be rewritten:

$$A_t = A_o e^{-k'_{obs} t} \tag{7}$$

Taking logarithms of this equation:

$$\log A_t = \log A_o - \frac{k'_{obs}}{2.303} t \tag{8}$$

$$\therefore \log A_t - \log A_o = - \frac{k'_{obs}}{2.303} t \tag{9}$$

Absorbances are calculated from % absorption indicated on photographs of oscilloscope traces, shown in the "Data Analysis" section of chapter III.

A plot of the logarithm of the change in absorbance vs. time will be a straight line if the reaction is first-order in solute concentration, and decays exponentially. The time when the maximum absorbance is halved is the half-life of the decay of e^-_{aq}. If $t_{1/2}$ is the half-life, equation (7) may be written as:

$$\frac{A_t}{A_o} = \frac{1}{2} = e^{-k'_{obs} t_{1/2}}$$

$$\therefore k'_{obs} = \frac{0.693}{t_{1/2}} \ s^{-1} \tag{10}$$

Equation (10) may be used to calculate k'_{obs}, the rate of decay of e^-_{aq}. The rate constant for the reaction of e^-_{aq} with solute molecules

(S) will be:

$$k_{obs} = \frac{0.693}{[S]\ t_{1/2}}\ M^{-1}\ s^{-1} \qquad (11)$$

The rate constant for the reaction of e^-_{aq} with small, freely diffusing molecules is greater than the rate constant with bulky molecules of low mobility (eqns. 2, 3). If the freely diffusing solute molecules are immobilised either by aggregating or becoming incorporated into a bulky biopolymer, the rate of reaction with e^-_{aq} will decrease. The change in the rate of e^-_{aq} decay with addition of a biopolymer to a solution of small molecules is a measure of the amount of molecular association. If there is no association, the reaction rate will simply be the sum of the rates of e^-_{aq} with solute and biopolymer alone. If association takes place, there will be a marked reduction in the reaction rate of e^-_{aq} when the biopolymer is added to the solute.

Oscilloscope traces of the exponential decay of e^-_{aq} absorption with time are used to find $t_{1/2}$, the half-life of the exponential decay. An estimate of the pseudo-first order rate and rate constant for the reaction of e^-_{aq} with the solute is then made using equations 10 and 11, respectively.

In the absence of a macromolecule, when there are only freely diffusing small solute molecules present, a reaction takes place at almost every encounter and the rate constant is $\sim 2 - 4 \times 10^{10}\ M^{-1}\ s^{-1}$. If macromolecules are introduced, with which the solute molecules associate, they will cease to diffuse freely and the probability of their encountering e^-_{aq} decreases dramatically. The e^-_{aq} lifetime is thus increased.

This change in the rate constant is used to monitor the degree and strength of binding of small molecules to macromolecules. The next section describes how binding parameters may be obtained from the reaction rate constants.

(d) Binding Assay

In studying the binding or association of molecules, the parameters of interest are the number of binding sites per molecule, n, the strength of the association (as measured by the association constant K) and factors that influence the interaction.

If P represents a molecule or ion containing n binding sites, each capable of attaching another molecule or ion A, and $\bar{\nu}$ is the number of occupied sites, then $\frac{\bar{\nu}}{n}$ is the fraction of all available sites occupied by molecules, and $1 - \frac{\bar{\nu}}{n}$ or f/n is the fraction of free sites. The interaction between P and A may be represented by the following equilibrium:

$$P + A \underset{k_{-1}}{\overset{k_1}{\rightleftharpoons}} P - A \text{ complex} \tag{12}$$

The extent of complex formation is determined by the forward and backward reaction rates:

$$\frac{d[P\text{-}A]}{dt} = k_1[P][A] - k_{-1}[P\text{-}A] = 0 \tag{13}$$

By the law of mass action, the association constant is given by

$$K = \frac{k_1}{k_{-1}} = \frac{[P\text{-}A]}{[P][A]} M^{-1} \tag{14}$$

If f_i represents the fraction of biopolymer (P) sites free of small molecules (A), then

$$f_i = \frac{[P]_{free}}{[P]_{free} + [P\text{-}A]} = \frac{1}{1 + K[A]} \tag{15}$$

If ν_i represents the fraction of bound sites, then,

$$\nu_i = (1 - f_i) = \frac{K[A]}{1 + K[A]} \tag{16}$$

If $\bar{\nu}$ now represents the number of moles of A bound per mole of macromolecule and the n sites are equivalent and independent then:

$$\frac{\bar{\nu}}{n} = \frac{K[A]}{1 + K[A]}$$

or, $$\frac{\bar{\nu}}{[A]} = K(n - \bar{\nu}) \tag{17}$$

This expression is used to draw a modified Scatchard plot (24). In order to relate these quantities to parameters found by pulse radiolysis, let k_p be the e^-_{aq} pseudo first order reaction rate constant with the polymer 'P' alone. k_A is the e^-_{aq} reaction rate constant with molecule 'A' alone. k_{obs} is the e^-_{aq} reaction rate constant when both 'P' and 'A' are present. The respective reaction rates are represented by k'_P, k'_A and k'_{obs}. In the absence of binding, the e^-_{aq} reaction rate will simply be $k'_{obs} = k'_P + k'_A$. If binding occurs, the reaction rate k'_{obs} will decrease. In this case k'_{obs} will be given by the following expression:

$$k'_{obs} = k_P[P_{unbound}] + k_{A_{bound}} [P_{bound}] + k_A [A_{unbound}] \tag{18}$$

B is a kinetic binding parameter proportional to $\bar{\nu}$, the molar fraction of bound dye. The parameter $\bar{\nu}$ (number of moles of dye bound per mole of macromolecule) is determined by spectroscopic methods in conventional studies of binding. The parameter B is the kinetic equivalent of $\bar{\nu}$ in pulse radiolysis studies, and is determined using kinetic changes in e^-_{aq} reactivity to indicate binding.

$$\therefore B = \alpha\bar{\nu} \tag{19}$$

α is a constant.

B can also be written as:

$$B = \frac{k'_P + k'_A - k'_{obs}}{k_A[P]} \tag{20}$$

In the absence of binding, $k'_P + k'_A = k'_{obs}$ and B becomes zero. For complete association, $B = \frac{[A_{bound}]}{[P]}$

Combining equation (17) and (19):

$$\frac{B}{[A_{unbound}]} = K(\alpha n - B) \tag{21}$$

This expression is used to draw a modified Scatchard plot (24). B may be obtained once the e^-_{aq} reaction rates have been calculated from the half-lives of e^-_{aq} decay using equation (20). $[A_{unbound}]$, the concentration of unbound solute, is equal to

$$[A_{unbound}] = \frac{(k'_{obs} - k'_P)[A]}{k'_A} \tag{22}$$

The slope of the modified Scatchard plot ($B/[A_{unbound}]$ vs B) is a measure of K, the association constant. This indicates the strength of the association. The intercept on the x-axis is αn where n is the number of binding sites per macromolecule. With $\alpha = 1$, good results have

been obtained for the binding of ethidium bromide to DNA (15) and acridine orange to DNA (see Results and Discussion). If the Scatchard plot is a straight line, the binding is relatively straight forward. One class of binding site is present. If the Scatchard plot is a curve, more than one class of binding site is apparent and binding at one site influences binding at another. A two-component curve indicates the presence of two classes of binding sites.

Chapter III

EXPERIMENTAL

a) Hardware

Nanosecond pulses of 3 MeV electrons were produced by the model KS-4000 Van de Graaff accelerator at the Whiteshell Nuclear Research Establishment. The electron source is a directly heated tantalum cathode. The pulse radiolysis system has been described by Hunt et al (47). A schematic diagram of the experimental set-up used in this laboratory is shown in figure 1.

Solutions under investigation were placed in a quartz cell that was aligned with the beam shutter, and illuminated by a 150 Watt xenon lamp. The lamp has a remote controlled shutter and an ultraviolet cut-off filter. The opening of the shutter is synchronised with the electron pulse from the accelerator, in order to avoid photolysis of light-sensitive solutions and damage to the photomultiplier tube.

A series of mirrors and an opening in the shielding of the accelerator room brought the analysing light out to the control room. Optical detection equipment is placed outside the accelerator room for convenience and to prevent interference from Čerenkov light and electronic noise. The analysing light is focussed onto a monochromator, which cuts off all wavelengths but 650 nm, and then passed on to the photomultiplier tube. The photomultiplier tube converts the light signal to an electrical signal, which is displayed on an oscilloscope screen and photographed.

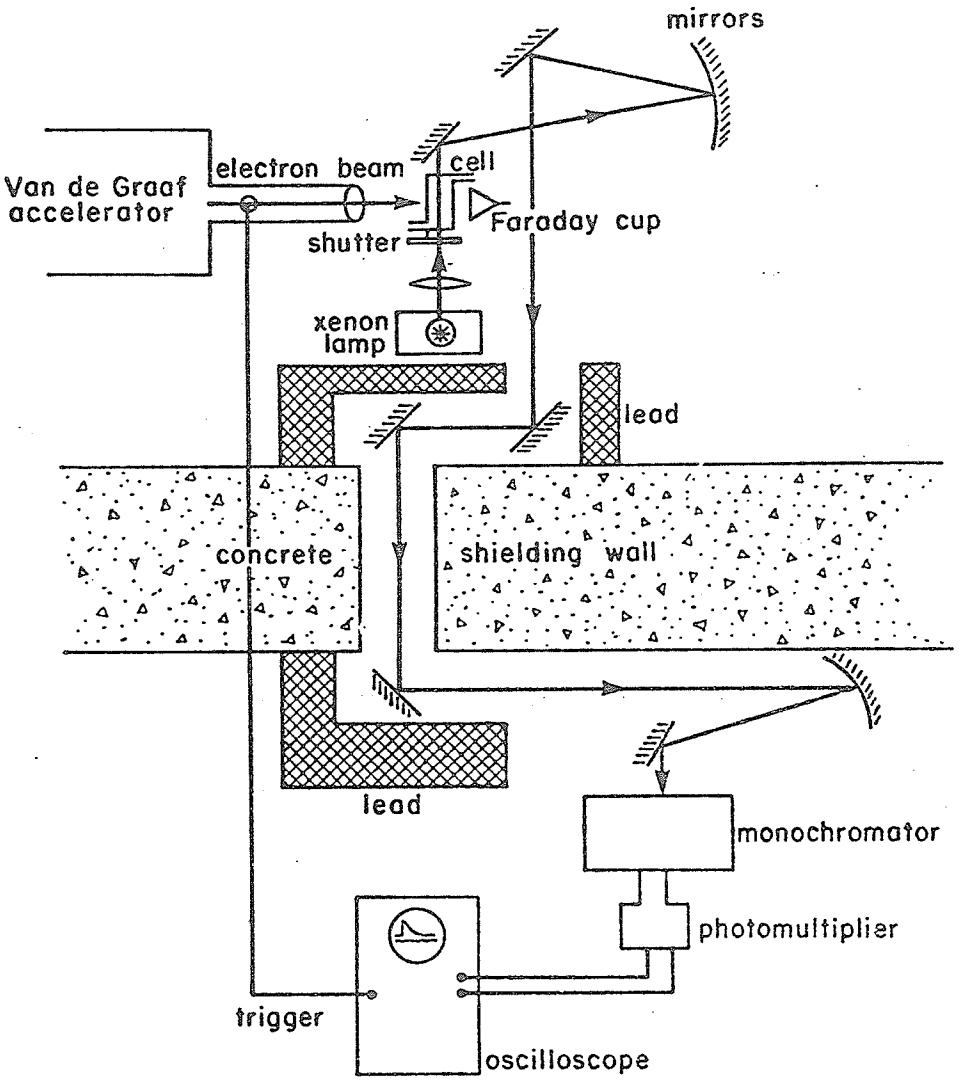

FIGURE 1. Schematic diagram of the nanosecond pulse radiolysis equipment.

Irradiating one sample at a time is a slow process. For greater efficiency, different solutions were placed in four syringes on a four-way valve driven by a selsyn motor (see figure 2). The valve outlet was connected to the cell with flexible tubing. The four-way valve could be manipulated from the control room (by remote control) and its operation was controlled by closed circuit T.V. In this way, four samples could be irradiated in rapid succession.

All glassware used such as syringes, pipettes and flasks was washed in chromic acid and rinsed three times with distilled water. Glassware was then placed in an oven for several hours to oxidise organic impurities by pyrolysis.

b) Sample Preparation

All solutions were prepared with triply distilled water. Solutions of dyes and other drugs were prepared immediately before use. DNA solutions were prepared 3 days before use and stored in the dark at 0°C. 0.1M t-butanol was added to all solutions, and the pH was adjusted to neutrality with the addition of KOH. Since e^-_{aq} reacts very rapidly with oxygen, all solutions were bubbled with high purity argon for 20 minutes immediately before use. This insured that the concentration of O_2 was below 10^{-6} M. At this oxygen concentration, e^-_{aq} takes 50 μs to react with it, which is ∿ hundred times slower than the reaction time of e^-_{aq} with solute molecules.

The DNA used was highly polymerized type I calf thymus DNA from Sigma Chemical Co. For experiments with heat-denatured DNA, DNA solutions were heated above 100°C, then cooled rapidly to 0°C and brought gradually

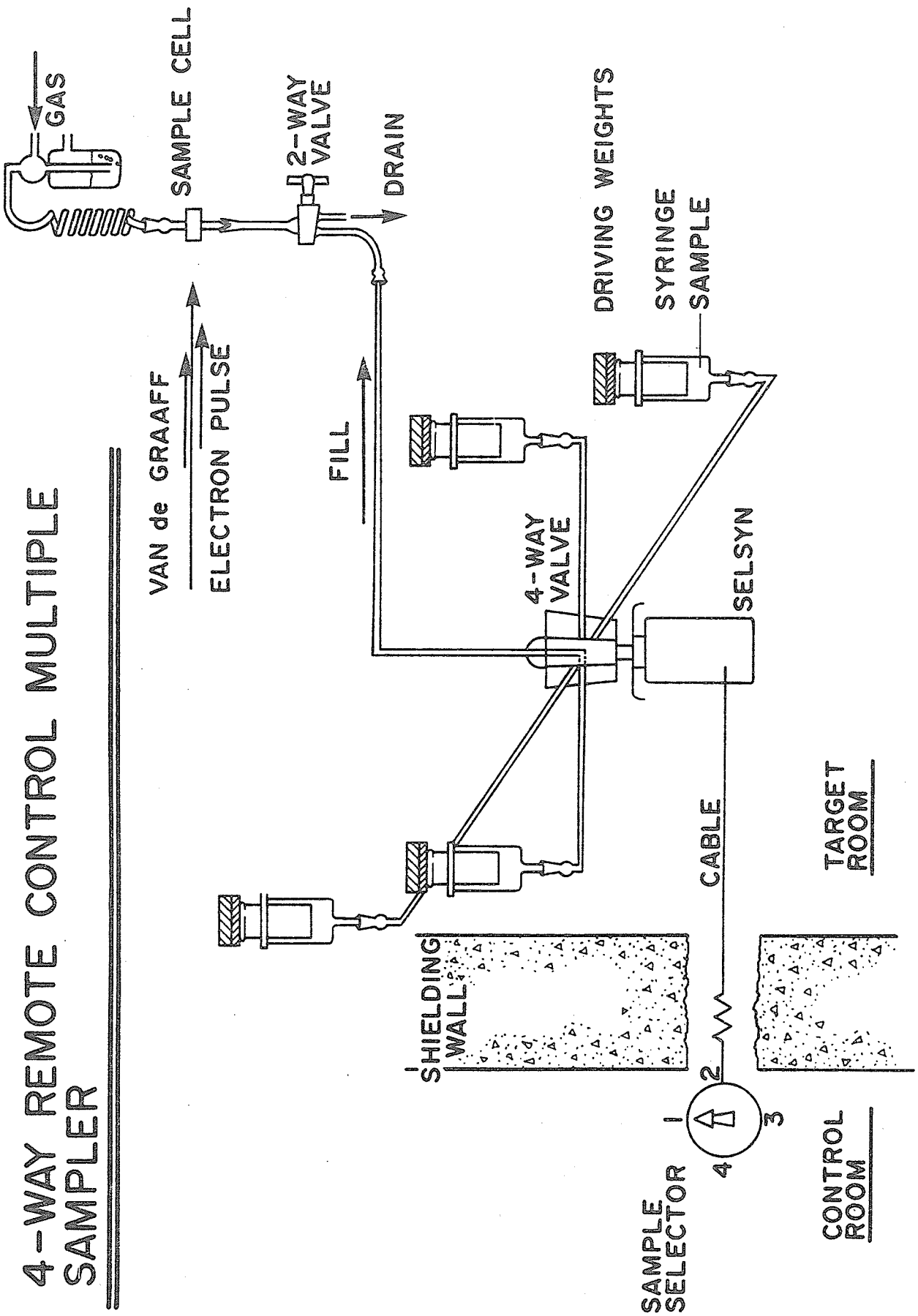

Figure 2: A multi-sample remote-control sample delivery system utilizing a selsyn motor driven 4-way valve.

to room temperature. This heat treatment completely uncoils the native DNA double helix, leaving intact single-stranded random coils. The absorbance at 260 nm was measured before and after heating. The observed 20-30 percent increase in absorption at 260 nm is due to hyperchromism and is evidence of denaturation.

In preparing the samples, great care was taken to minimize traces of impurities and oxygen. The e^-_{aq} reacts quickly with impurities and oxygen, and slowly with polynucleotides. The e^-_{aq} decay time can be affected greatly if small amounts of impurities are present.

c) Data Analysis

Data were obtained in the form of photographs of oscilloscope traces of the exponential decrease in absorption of e^-_{aq} with time. A typical trace is shown in figure 3. The photographs are used to measure absorbances. These may be measured manually, but this is a slow, inaccurate method. A computer program PULSER (49) has been developed (see Appendix) to analyse the data. The decay curve is traced by a graphic digitizer. Points on the curve are translated into "x" and "y" coordinates and these numbers are placed on magnetic tape. The first part of the program (Digitizer Translator Subprogram) converts these coordinates into millivolts and time, and stores them on dectape for the Data Analysis Subprogram. This subprogram determines if the transient is a simple decay, carries out the kinetic analysis and prints out the results. The program uses the PDP10 computer at WNRE.

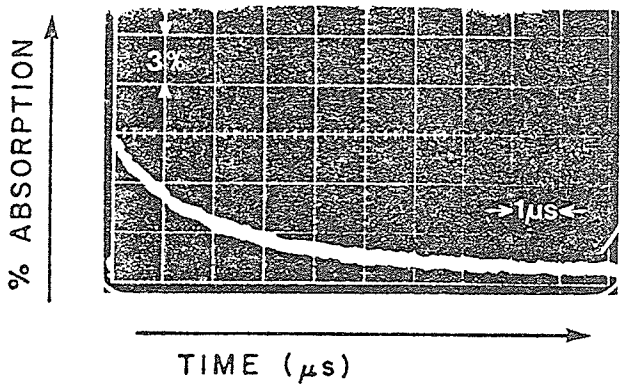

Figure 3: A typical oscilloscope trace showing the first-order exponential decay of e^-_{aq} absorption at 650 nm. Dose per pulse ∿1.5 krad. Deoxygenated aqueous solution containing 10^{-5}M EB and 0.1 M t-butanol as an .OH-scavenger.

d) Experimental Errors

Random errors may be introduced due to the presence of impurities in the samples. These were minimised by thorough cleaning of glassware used, as described in Chapter III, Section a). Solutions were prepared with triply distilled water, and all samples were carefully weighed. Solutions of dyes and drugs were prepared immediately before use and DNA solutions were stored at $0^{o}C$. High purity argon or nitrogen was bubbled through each solution for 30 minutes to remove all traces of dissolved oxygen, and t-butanol was added to remove $\cdot OH$ radicals. However, once these sources of statistical error have been minimised, inaccuracies in experimental results arise because hydrated electrons react with each other. As they diffuse away from their point of origin, not only do they react with impurities, oxygen and $\cdot OH$ radicals, but also with other hydrated electrons they may encounter. These competing reactions become significant when the solute concentration is low. The hydrated electrons traverse a greater distance before encountering solute molecules and have a higher probability of reacting with other products of radiolysis. This is the major source of systematic error.

Typical doses of 1 krad are generated by 50 ns pulses of 3 MeV electrons from the Van de Graaff accelerator. This results in an instantaneous concentration of 3μM of e^{-}_{aq} . Hydrated electrons react with each other by the following mechanism:

$$e^-_{aq} + e^-_{aq} \xrightarrow{2H_2O} H_2 + 2OH^- \qquad (23)$$

The rate constant for the reaction is of the order of 10^{10} $M^{-1}s^{-1}$ (11). With a high solute concentration, the probability of the above reaction taking place is reduced considerably . This is the most outstanding source of experimental error. In the calculation of the reaction rate the error is estimated to be of the order of $\pm$ 10% to 20%.

Errors were probably incurred in tracing the exponential decay curves on the photographs, with the graphic digitizer. These errors, of the order of $\pm$ 2%, are small compared with the error due to the possible combination of hydrated electrons with each other.

Three photographs were obtained for each concentration of solute used. The average value of the reaction rate was obtained, and these values used to find the binding parameters.

All these errors are shown by error bars on Figures 1 to 16.

Chapter IV

RESULTS AND DISCUSSION

a) Interaction of Acridine Orange with DNA

The interaction of acridine orange and DNA was investigated in depth using the pulse radiolysis binding assay. The concentrations of DNA used were 0.01% and 0.02%, which correspond to effective nucleotide (MW = 350) concentrations of 2.9×10^{-4} M and 5.8×10^{-4} M, respectively. The acridine orange concentration ([AO]) was increased from 5×10^{-5} M to 2×10^{-4} M, in order to cover the range of strong and weak interactions of ligand and macromolecule at neutral pH. At higher acridine orange concentrations the molecules have a tendency to form dimers, or aggregates.

Semilog plots were drawn for the exponential decay of e^-_{aq} absorption at 650 nm, in the presence of dye and macromolecule separately and together, at different concentrations. These semilog plots were used to measure the half-life ($t_{1/2}$) of the exponential pseudo-first order decay of e^-_{aq} absorption.

The reaction rate k' (s^{-1}) = $\frac{0.693}{t_{1/2}}$ and absolute rate constants $k = \frac{0.693}{t_{1/2}[AO]}$ M^{-1} s^{-1} were then calculated. These quantities were used to draw a modified Scatchard plot.

Test runs were first conducted to study the feasibility of investigating this interaction by the pulse radiolysis method. These results have been published (50). The rate constant obtained for the reaction of e^-_{aq} with dye alone was of the order of 2.5×10^{10} M^{-1} s^{-1}.

Similar results but studying only qualitatively, drug -protein interactions, have been obtained by J.D. Buchanan (51) for the rates of decay of e^-_{aq} absorption at 650 nm with the aminoacridines proflavine, benzoflavine and acridine orange.

Figure 4 shows the reaction rates for AO alone, and AO in the presence of 0.02% DNA, with an error of $\pm$ 10% - 20%. This error is due to competing reactions of e^-_{aq} with other hydrated electrons. Also at higher concentrations of AO, the AO molecules aggregate. This self-aggregation probably causes the rate to be low at high AO concentrations. The highest point on the graph (fig. 4) is probably low due to this experimental artefact. The initial slope, therefore, yields the most accurate rate.

There is a marked reduction in the reaction rate on addition of DNA to the AO solution. This is to be expected because, in the absence of binding, the reaction rate would simply be the sum of the rates with DNA and AO alone. However, when the dye is bound to DNA it is effectively immobilised and its e^-_{aq} reactivity, being essentially diffusion controlled, is decreased. On complete association, with no free dye remaining in solution, the observed e^-_{aq} reactivity (k'_{obs}) will be essentially equal to the rate of decay with DNA alone.

On addition of 5×10^{-5} M AO to 0.02% DNA, there should be complete association. At this dye to polymer ratio, energetically strong binding occurs, saturating at a dye to nucleotide ratio of 0.1. The binding energy is of the order of 6 - 10 kcal $mole^{-1}$ of aminoacridine bound (52). On increasing the concentration of AO, once the primary

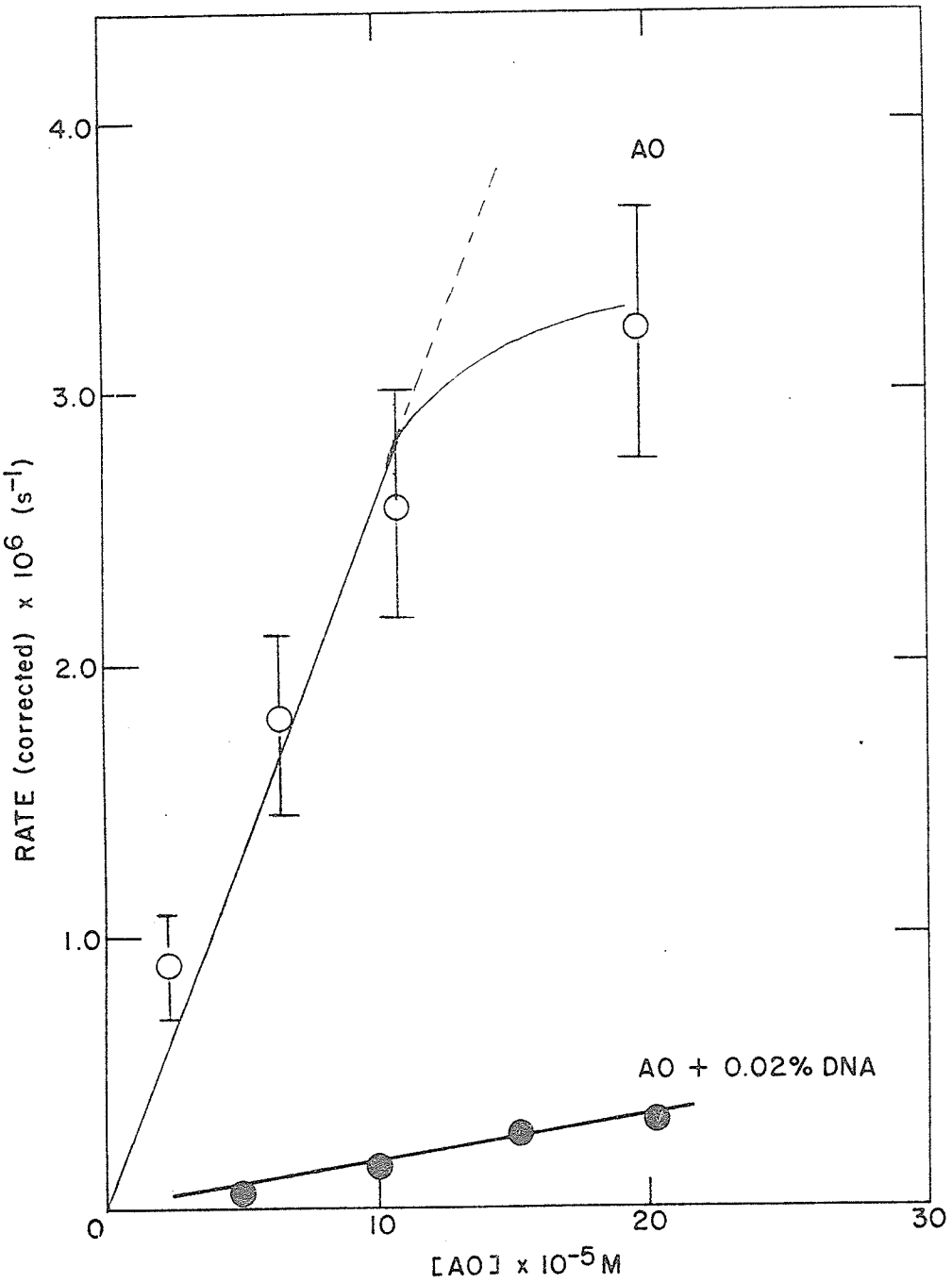

Figure 4: The decay of e^-_{aq} absorption at 650 nm as a function of AO concentration. Addition of DNA results in a marked decrease in e^-_{aq} reactivity towards AO, indicating complex formation between AO and DNA. The corrected rate is the observed rate less the natural rate of reaction of e^-_{aq} in solutions containing no substrate.

binding sites have been saturated, an energetically weaker secondary binding takes place (53), of the order of at most a few kcal $mole^{-1}$ of bound aminoacridine (51). The planar polycyclic dye molecules (fig. 8) both intercalate the grooves of the DNA helix, and are attached to the exterior of the helix at high dye concentrations. The attachment to the exterior of the polyanionic double helix is due to electrostatic attraction of the cationic dye molecules (Fig. 5a). The positive ring nitrogens are close to the phosphate groups of the DNA chain, the planes of the molecules being parallel to the bases (52). The planar AO molecules, however, have a tendency to aggregate (54) by stacking on top of each other, in the same direction as the helix axis. They interact mutually in a direction perpendicular to their aromatic planes and pile up on top of each other. This weak binding process is therefore not entirely electrostatic (23), the binding of one molecule facilitating the attachment of others. Difficulties arise in studying the AO-DNA interaction at high AO concentrations because these stacked molecules cannot be accomodated by intercalation, but cluster around the exterior of the DNA helix.

The aggregation of AO molecules and the AO-DNA interaction have been investigated by a number of techniques including NMR and optical spectroscopy. NMR is useful in elucidating the structure of the complexes. It is possible to determine the orientation of the DNA base-dye complex by following the proton chemical shifts as a function of dye concentration.

A coplanar arrangement of dye molecules and DNA base rings would result in a down-field shift of base protons. However, upfield shifts of base protons have been observed (55) with increasing dye concentration.

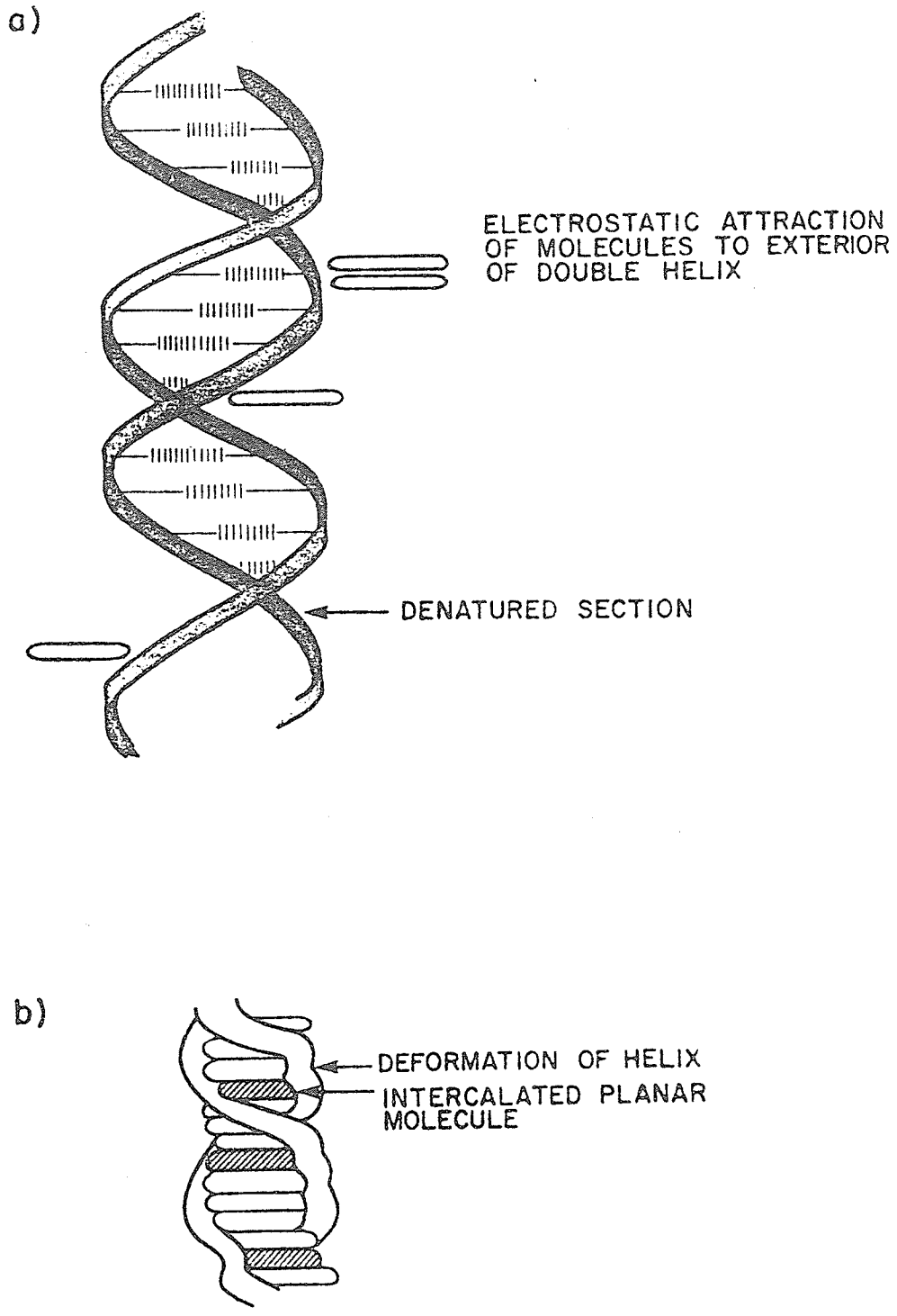

Figure 5 a) Planar polycyclic dye molecules attached by electrostatic attraction to the exterior of the DNA double helix.

b) Intercalation of planar polycyclic dye molecules into the DNA double helix by extension and deformation of the DNA back-bone.

Proton chemical shifts in the NMR spectra of AO on dilution have been measured (36). The ring and N-methyl protons shift to low field markedly on dilution. The ~50-fold deshielding is attributed to the breaking up of large aggregates of AO molecules. There are also large changes in the chemical shifts for the 3,4 and N-CH_3 protons. Results suggest that the most probable orientation of adjacent AO molecules is one in which the 1,9 and N-CH_3 protons are located nearly over the centre of adjacent rings. This type of structural information may be useful in designing model DNA intercalants for specific bacteriostatic, mutagenic or radiosensitizing action. The interaction, its strength, and the number of binding sites can be obtained rapidly by pulse radiolysis.

The pulse radiolysis technique verifies, simply and rapidly, that the interaction takes place, by monitoring the lifetime of e^-_{aq}. In addition to this, quantitative information on the interaction may be obtained, as detailed later in this chapter. Binding curves reveal the number and strength of binding sites.

No single method, however, yields enough information to elucidate completely the mechanism of a molecular interaction. X-ray diffraction patterns of fibres of the complex with proflavine show changes in the usual helical structure of DNA (43). Disappearance of the characteristic layer-line pattern suggests a disordering of the helical backbone. Stiffening of the DNA molecule on complex formation with acridines and a resultant increase in viscosity and change in sedimentation coefficient have been used to obtain binding curves (43).

Lerman first proposed a model for the strong binding (43,58). He envisaged intercalation of an aminoacridine molecule between adjacent base pairs on the DNA chain, facilitated by extension and unwinding of the deoxyribose phosphate backbone (fig. 5b). The helix length increases by 3.4 Å for each intercalated molecule, the plane of the aromatic triple rings being perpendicular to the helix axis. The molecule is stabilised by electrostatic forces and London-Van der Waals forces between aminoacridines and neighbouring base pairs due to the overlapping of their π-electron orbitals. Figure 6 shows the triple aromatic rings superimposed on the DNA bases.

Figure 7 is a modified Scatchard plot of the binding of AO to DNA. B is the kinetic binding parameter such that

$$B = \frac{(k_{AO}[AO] + k_{DNA}[DNA] - k'_{obs})}{k_{AO}[DNA]} \qquad (20a)$$

where k_{AO} and k_{DNA} are the e^-_{aq} reaction rate constants with AO and DNA alone, respectively, and k'_{obs} is the observed reaction rate with AO and DNA combined. The equation $\frac{B}{[AO]_{free}} = K(n - B)$ was then used to construct the modified Scatchard plot. A straight line would indicate the presence of one type of binding site and yield one association constant. A two-component curve shows the presence of two classes of binding site. A curved region on the graph indicates the overlapping of two types of binding sites. The initial section of the graph is linear and gives an intercept of 0.1 on the X-axis. This is equal to the dye to site ratio for strong binding, and is in agreement with results obtained by more conventional methods. Under conditions where the binding efficiency is low, considerable error is associated with the determination of $B/[AO]_{free}$, and this introduces large variations in the value of K. The initial negative slope of the curve, $K \sim 5 \pm 2 \times 10^5 (M^{-1})$

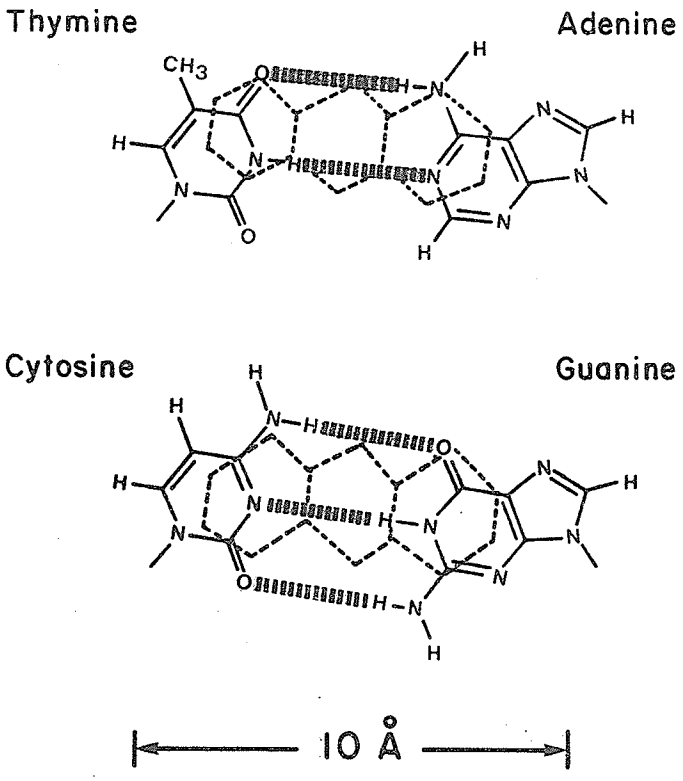

Fig. 6: Triple aromatic rings superimposed on the DNA bases.

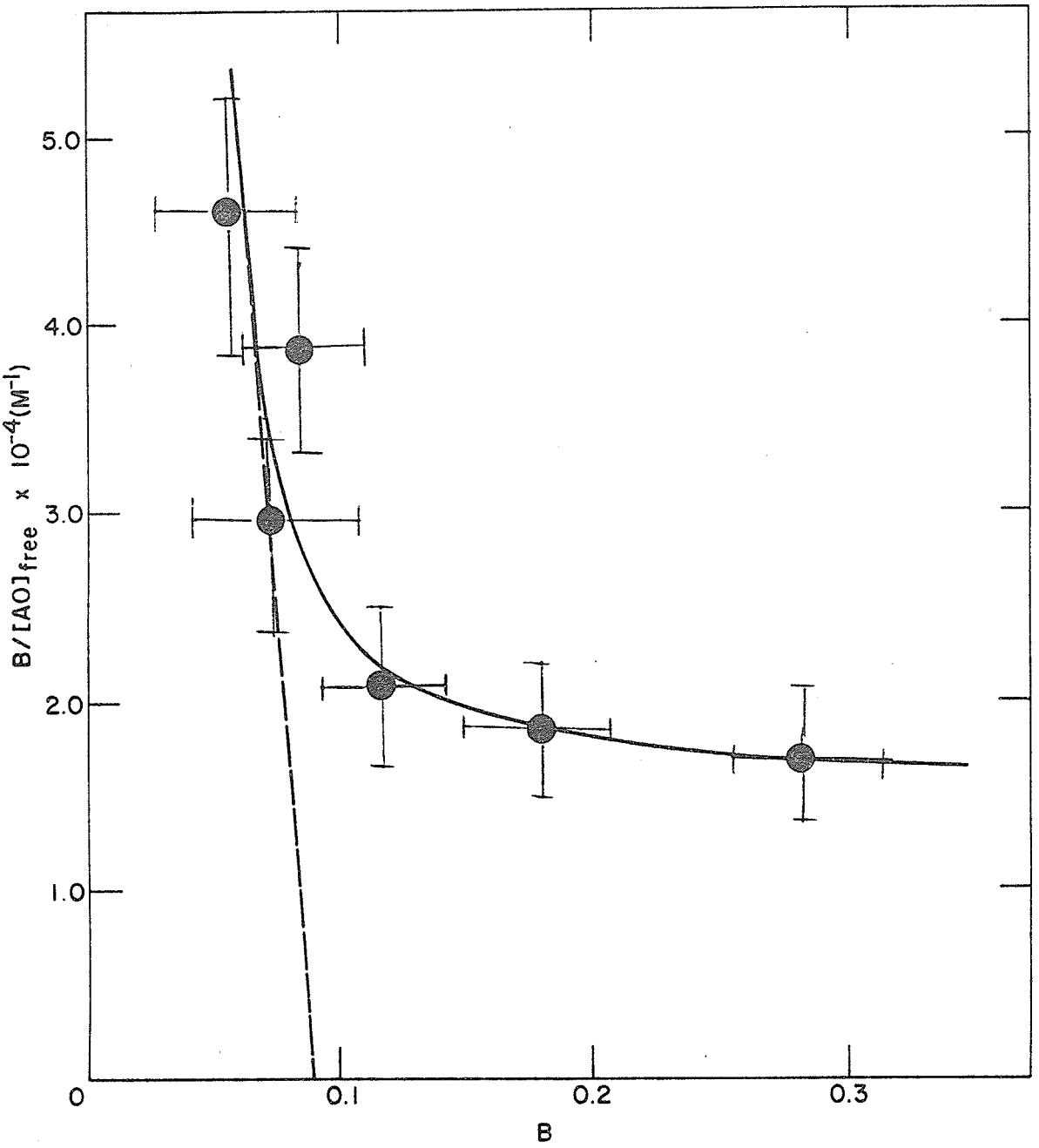

Figure 7: A Scatchard-type plot for the binding of AO to DNA. The negative slope of the line is a measure of the association constant $K(M^{-1})$. The AO concentration was varied from 10^{-5}M to 4 x 10^{-4}M and the DNA concentration from 0.1% to 1%.

is a measure of the association constant for strong binding. The slope gradually decreases with increasing AO concentration. This type of analysis has been used successfully to measure the association constant and other binding parameters for the ethidium bromide-DNA interaction(15), and the dinitro-EB-DNA interaction (50). Curvature of the graph shows the overlapping of binding sites. The association constant is changing. Once the primary sites, or sites for intercalation, are filled, the AO molecules attach themselves to the exterior of the double helix at the secondary sites. However at higher values of the binding parameter B, the concentration of AO is greater, and due to the stacking of AO molecules the secondary sites are not all equivalent. One AO molecule facilitates the stacking of another. The binding of AO to DNA is, therefore, fairly complicated. The latter portion of the curve at high AO concentrations is not linear. The presence of clumps (i.e. stacks) of AO molecules affect the rate of decay of e^-_{aq}, leading to some degree of error in the calculation of the binding parameter B. A tangent to the latter portion of the curve will yield the association constant.

It has also been observed that AO binds preferentially to A-T rich regions of DNA, and less to G-C rich regions (57). This heterogeneity of binding sites is reflected in a curved Scatchard plot.

The interaction of DNA and the aminoacridines has been studied extensively not only because of their mutagenic and bacteriostatic action, but also because they resemble structurally the carcinogenic benzacridines and polycyclic hydrocarbons. An aminoacridine with an electron-affinic side chain would be a potential radiosensitizer. Though strong binding is considerably reduced when 9-amino-1,2,3,4-tetrahydroacridine is combined with DNA (58) due to the bulky nature of one of the rings, binding is not reduced when long bulky side chains are attached to the 9-amino group as in atebrin (see figure 8). Atebrin has been found to increase the radiosensitivity of bacteria (malaria plasmodia) (59). The toxicity of this aminoacridine, however, at doses necessary to achieve radiosensitivity, limits the use of this particular compound in mammalian cells.

A number of macromolecules were rapidly screened for their interaction with AO. A low (corrected*) rate on combining macromolecule with AO indicates some form of complex formation. Whereas binding occurs with chondroitin sulfate ($ChSO_4$) and myoglobin, there is minimal binding with the neutral molecules of bovine serum albumin (BSA).

* The rate was corrected for the finite e_{aq}^- lifetime in a solution containing the macromolecule only.

Table 2

Kinetic Parameters for the Interaction of Acridine Orange with Various Macromolecules

Molecules present	Corrected rate x 10^6 (s^{-1})*
Acridine orange 10^{-4}M	4.2
AO10^{-4}M + DNA .04%	1.2
AO10^{-4}M + $ChSO_4$ .02%	1.4
AO10^{-4}M + Myoglobin .02%	0.4
AO10^{-4}M + BSA .01%	4.1

* $k'_{AO\ corr} = k'_{obs} - k_{DNA}[DNA]$

The interaction of acridines and nucleic acids is assumed, in many cases, to be the cause of the biological effects of the acridines. Their ability to extend and stretch polynucleotide chains of DNA may lead to additions or deletions in the genetic code (59) or stabilization of DNA against strand separation at the point of intercalation. In either case, the result may be mutagenesis or carcinogenesis. In vivo, the rate of formation of the complex may be significant.

It is important, therefore, to determine the factors that affect these complexes, by changing parameters such as the ionic strength, temperature or structure of macromolecule or ligand. It has been found that an increase in ionic strength diminishes secondary binding to a greater extent than primary binding of AO to DNA (60).

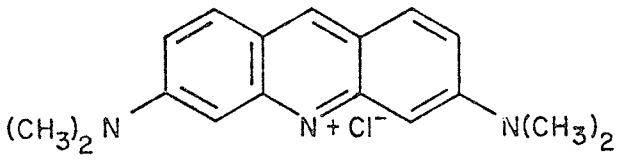

ACRIDINE ORANGE

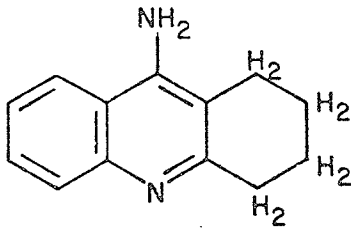

9-AMINO-1,2,3,4-
TETRAHYDRO-ACRIDINE

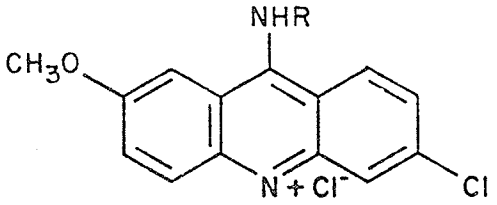

ATEBRIN (QUINACRINE)

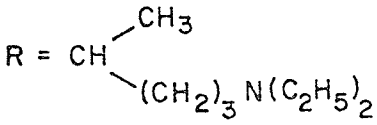

Figure 8: Chemical structures of Acridine Orange and some of its derivatives.

The mutual repulsion of acridinium cations appears to be the main factor limiting primary binding (61). Thermodynamic factors involved in the binding of AO to native and heat-denatured DNA have been obtained by extensive equilibrium dialysis studies (62). AO was released at a greater rate from denatured DNA than from native DNA as the temperature was increased above 20°C. Presumably the secondary structure of denatured DNA is destroyed at a greater rate with increasing temperature.

It is shown in the following sections that pulse radiolysis can be effectively used to study the effects of changes in the structure of macromolecules and changes in ionic strength, on the binding of small molecules.

b) Conformational Changes in Macromolecules

The biological action of a drug that interacts with a biopolymer is generally assumed to be due to conformational changes induced in the biopolymer on binding. Pulse radiolysis has been used successfully to study conformational changes induced by pH (9), temperature (63) and drugs (14). Conformational changes in proteins may reduce the availability of cationic sites on the protein molecules for the hydrated electron. Variations in reactivity towards the hydrated electron are, therefore, a measure of the degree of conformational change in the biopolymer.

Generally, a definite secondary structure in the macromolecule is required for a drug to bind to it. Lack of this secondary structure results in a greater concentration of the drug in the free state. The

rate of disappearance of e^-_{aq} is a monitor of the amount of drug bound and in the free state. Measurements of the reaction rates of e^-_{aq} in the presence of drug and macromolecule can therefore be used to determine the degree of conformational change in the macromolecule.

Drugs such as acridine orange, that have a planar aromatic ring structure, bind polynucleotides essentially through hydrophobic interactions by the insertion of the aromatic ring between the stacked bases of the polynucleotide. The trypanocidal dye ethidium bromide (EB) requires the base-paired helical structure of DNA in order to bind to it strongly (21). The planar phenanthridine ring of EB intercalates between adjacent base pairs on the DNA helix. This interaction has been studied extensively by conventional methods (21, 64) and by pulse radiolysis (15). It has been found that strong primary binding occurs at sites that are saturated when the drug to nucleotide ratio is $\sim$0.2. At higher drug concentrations an additional weaker secondary binding takes place, and saturation occurs when the drug to nucleotide ratio is 1.0 (21). Secondary binding is due to electrostatic attraction of the positively charged EB molecules to the exterior of the polyanionic helix (65).

Because of the electrostatic nature of the secondary binding, addition of salts such as $MgCl_2$ to the EB-DNA medium causes a reduction in the strength of the interaction (22). There appears to be some release of EB from sites on DNA when $MgCl_2$ is added, as the rate of e^-_{aq} decay increases. This is shown in Table 3. The effect seems to be due to some EB displacement and not simply the reaction of e^-_{aq} with $MgCl_2$.

Table 3

The Effect of Salts on the Rate of Decay of e^-_{aq} with EB and DNA

Small Molecules and Biopolymer	Rate of e^-_{aq} Decay x 10^6 (s^{-1})
0.1 mM EB	3.6
0.1 mM EB + .01% DNA	1.1
0.1 mM EB + .01% DNA + .05M $MgCl_2$	2.0
0.05 M $MgCl_2$	0.6
0.1 mM EB + .02% DNA	1.0
0.1 mM EB + .02% DNA + 0.5M $MgCl_2$	3.3
0.5 M $MgCl_2$	1.0

Waring originally reported that DNA, denatured by heating and rapid cooling, exhibited the same type of binding with EB as duplex DNA (21). However, by also raising the pH of heat denatured DNA from 8 to 12, a marked decrease in primary binding occurs (66). The increase in pH prevents the formation of short duplex regions by intramolecular hydrogen bonding. The pulse radiolysis method was used to investigate the degree of conformational change in heat denatured DNA.

Calf thymus DNA was denatured by heating beyond the thermal transition temperature for DNA denaturation or "melting", followed by rapid cooling to 0°C. With DNA from eukaryotic cells, very few of the single strands should reassociate, since diffusion of the DNA strands is inhibited at low temperatures and it is difficult to match the complex base sequences. However, it appears that on cooling, some renaturation inevitably takes place by intramolecular hydrogen bonding. The amount of EB free in solution when duplex DNA is present, compared with the amount of EB free in solution when denatured DNA is present, is a quantitative measure of the degree of denaturation or conformational change, of DNA.

Figure 9 shows the effect of adding 10^{-4} M EB to .01% E-coli DNA ($\sim 10^6$MW), calf thymus DNA ($1.5X10^7$MW) and denatured DNA. The least amount of EB is bound to denatured DNA, as expected. E-Coli DNA allows more EB to bind than calf thymus DNA. This indicates either a greater degree of helical structure in E-Coli DNA, or that electrostatic binding is facilitated by the presence of more negative charge on the DNA molecules.

In order to study the interaction of EB and denatured DNA, .01% DNA, both duplex and denatured, was used. The concentration of EB

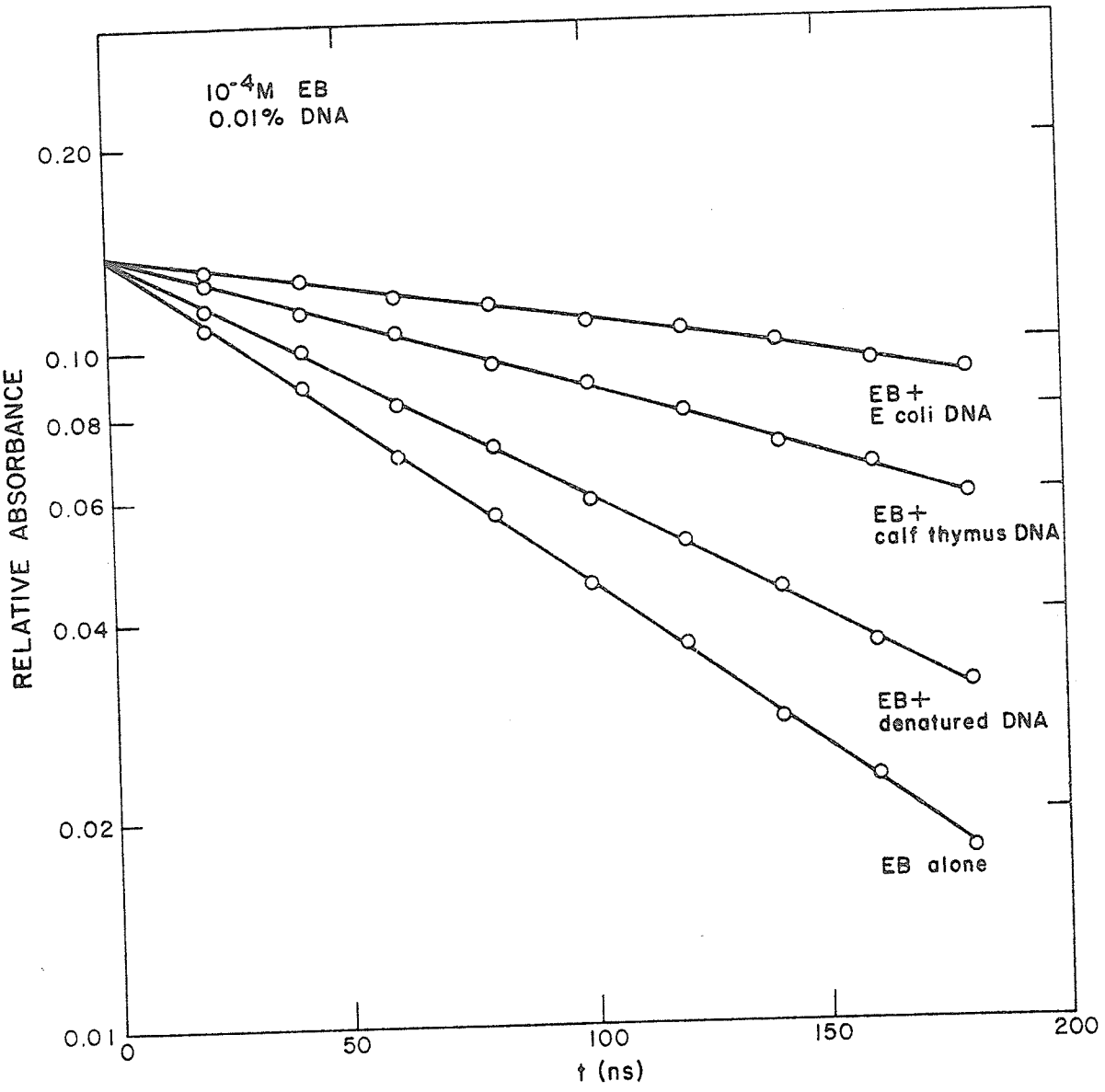

Figure 9: The effect of added calf thymus DNA, E-coli DNA and denatured DNA on the rate of reaction of e^-_{aq} with EB. The EB concentration was varied from 2×10^{-5}M to 4×10^{-4}M, while the DNA concentration was .01%. The pH of the solution was 6.0. Decrease in helical structure (as in denatured DNA) results in an increase in the concentration of EB free in solution, and an increase in the rate of reaction of e^-_{aq} with EB.

was varied from 10^{-5} M to 4 x 10^{-4} M. Results are shown in figure 10. The concentration of EB free in solution was calculated using the expression:

$$[EB]_{free} = \frac{(k'_{obs\ (corrected)} - k'_{DNA})[EB]}{k'_{EB}} \qquad (22a)$$

With duplex DNA, at low dye to nucleotide ratios, there is very little free EB. With increasing quantities of EB, both primary and secondary binding sites are filled and the concentration of EB free in solution increases. With denatured DNA, however, there is a greater concentration of EB free in solution at low dye to nucleotide ratios. When the EB concentration is 2.9 x 10^{-4}M and the dye to nucleotide ratio is 1, there is 11% more EB free with denatured DNA than with duplex DNA.

In order to investigate this further, a modified Scatchard plot showing the binding of EB to denatured DNA was drawn (figure 11). Here a two component curve is evident. The initial slope is $\sim 1.1 \pm 0.4 \times 10^6$ and the X-intercept is 0.1. The association constant, $K = 1.1 \pm 0.4 \times 10^6 M^{-1}$, indicates strong binding. However, the dye to nucleotide ratio of 0.1 is fifty percent less than the ratio for saturation of primary sites with duplex DNA, which is 0.2 (21). Also, at low dye to nucleotide ratios the Scatchard type plot indicates secondary binding. It appears, therefore that short sections of denatured DNA have paired to form some duplex regions.

In order to verify more directly by the pulse radiolysis method, this lack of primary binding when the helical secondary structure of

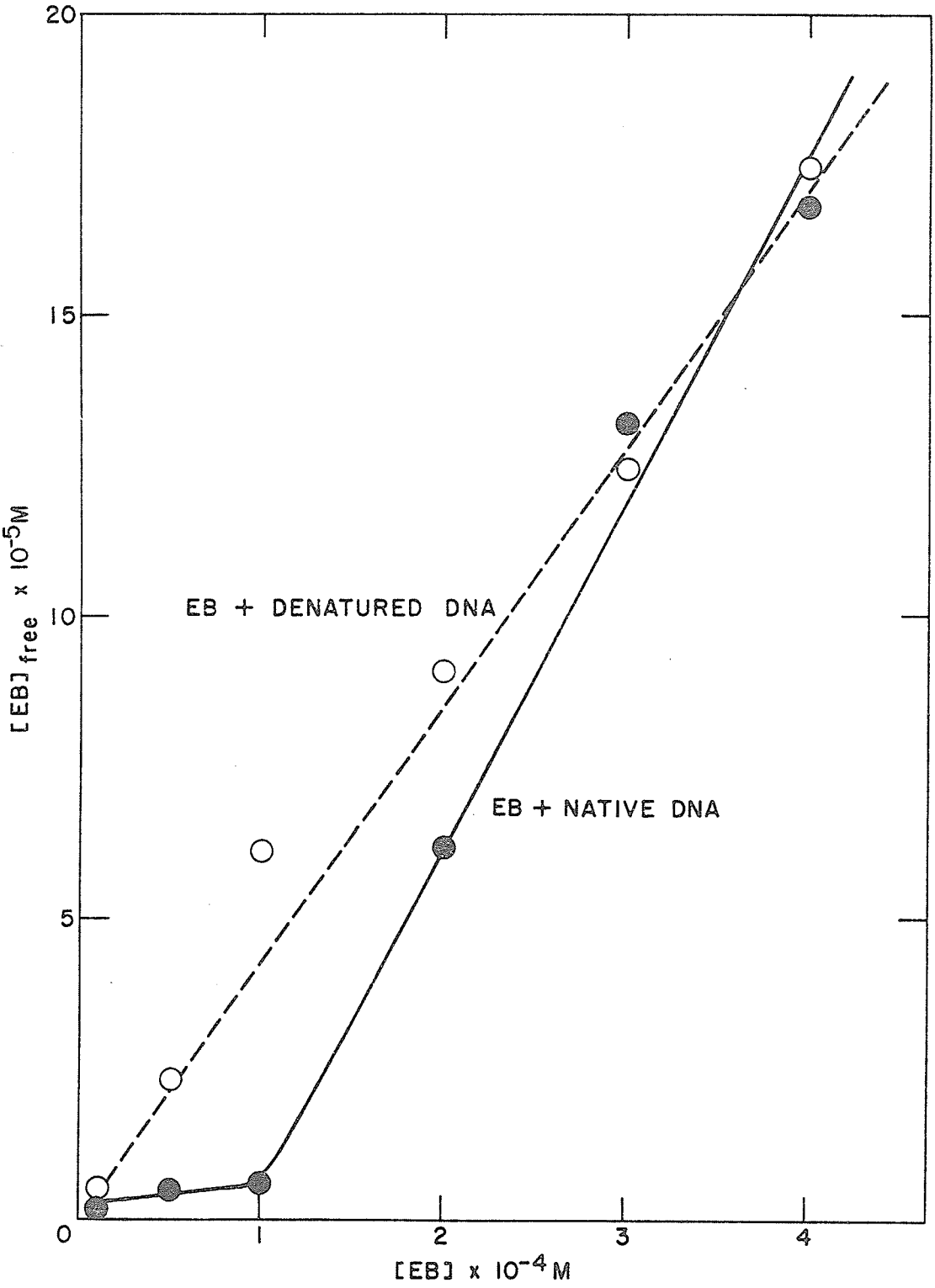

Figure 10: The concentration of EB free in solution when denatured DNA and native DNA is added to increasing concentrations of EB. The EB concentration was increased from 0.5 x 10^{-4} M to 4 x 10^{-4} M and the DNA concentration was .01%.

Figure 11: A modified Scatchard plot for the binding of EB to denatured (random coil) and native (helical) DNA.

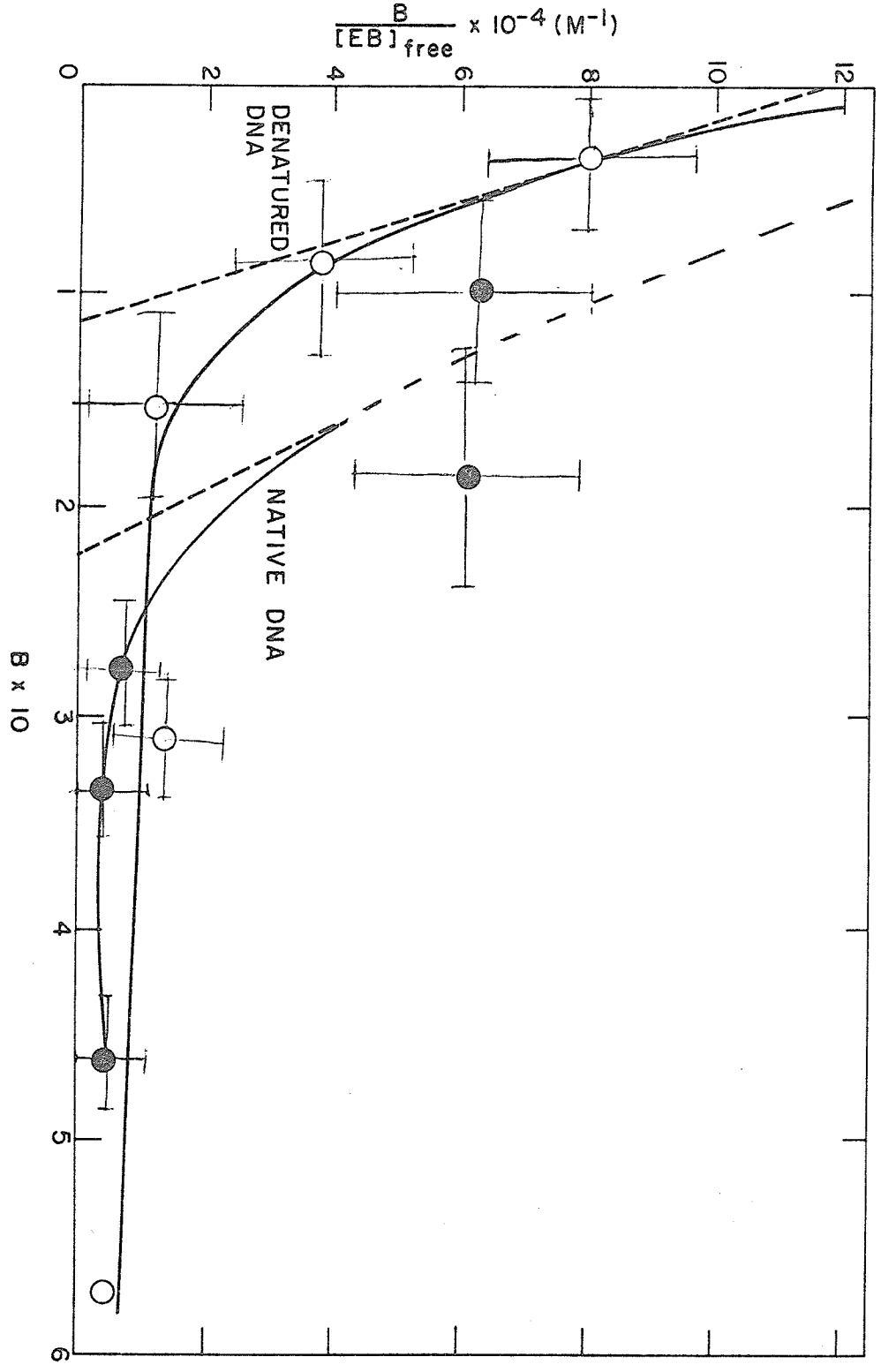

nucleic acids is absent, the interaction of EB with the synthetic homopolymers polyguanylic acid (poly G) and polyuridylic acid (poly U) was investigated. Poly U exists in aqueous solution largely as nonhelical random coils (67). Poly G has a four-stranded structure (68). Binding curves obtained by conventional optical methods (64) reveal the presence of only one type of binding site on these homopolymers. Figures 12 and 13 are modified Scatchard plots for the interaction of EB with poly G and poly U, respectively. The homopolymer concentration was kept constant at 0.01%. The EB concentration was varied from 10^{-5} M to 4 X 10^{-4} M.

Both Scatchard plots are linear, indicating the presence of one type of binding site on the homopolymers. The association constant in the case of poly G is 2.5 X 10^{4} M^{-1}, and for the poly U - EB complex is 3.1 X 10^{3} M^{-1}. These low values indicate weak secondary binding of EB to both poly G and poly U, though the poly G interaction is stronger. It seems likely, therefore, that the cationic EB molecules are attracted mainly by electrostatic forces to the negatively charged phosphates of the homopolymers. There is considerable scatter in the data points in figure 13. This could be due to some form of base stacking and unstacking, with an absence of a hydrodynamically rigid structure (69), present in poly U. The absence of strong primary binding or intercalation of EB to these polynucleotides, however, shows little evidence, if any, of double helical formation in solution.

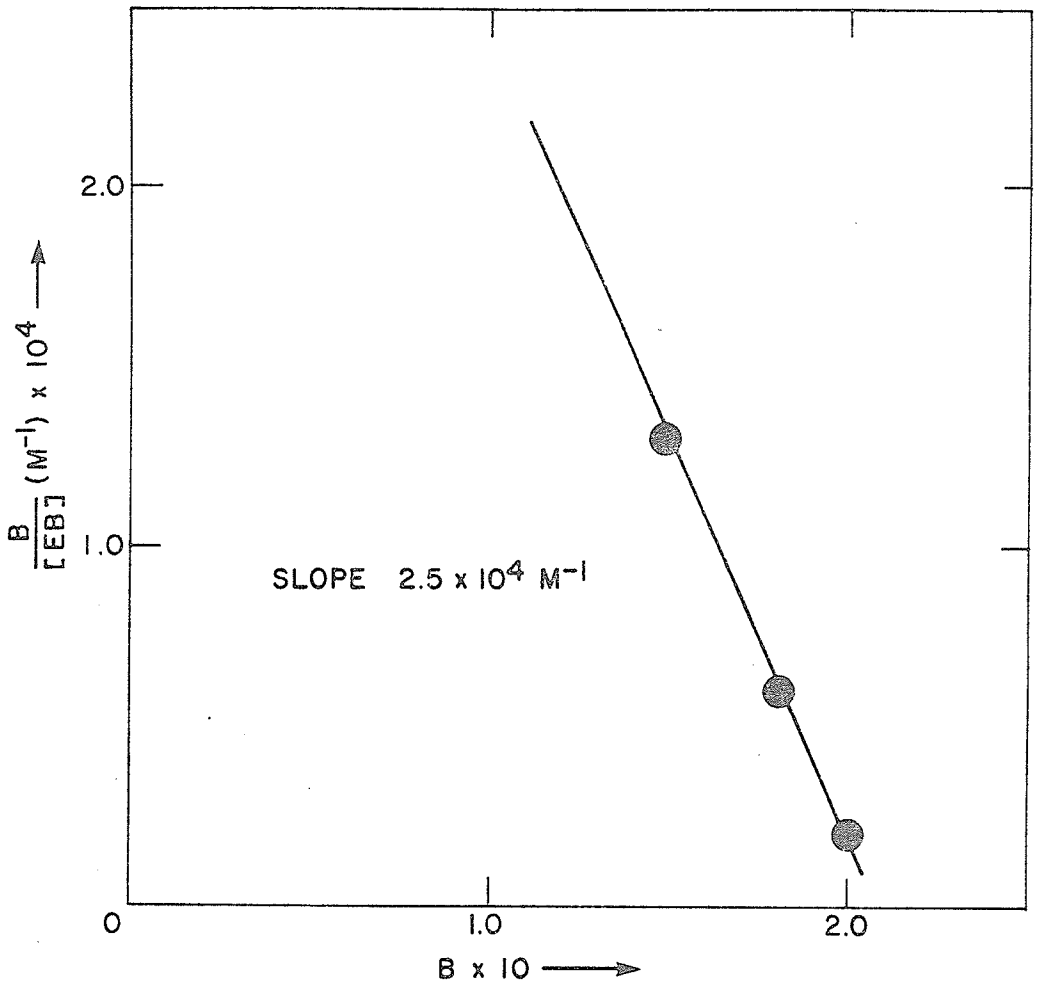

Figure 12: A Scatchard type plot for the binding of EB to poly G. One class of binding site is indicated by the straight line.

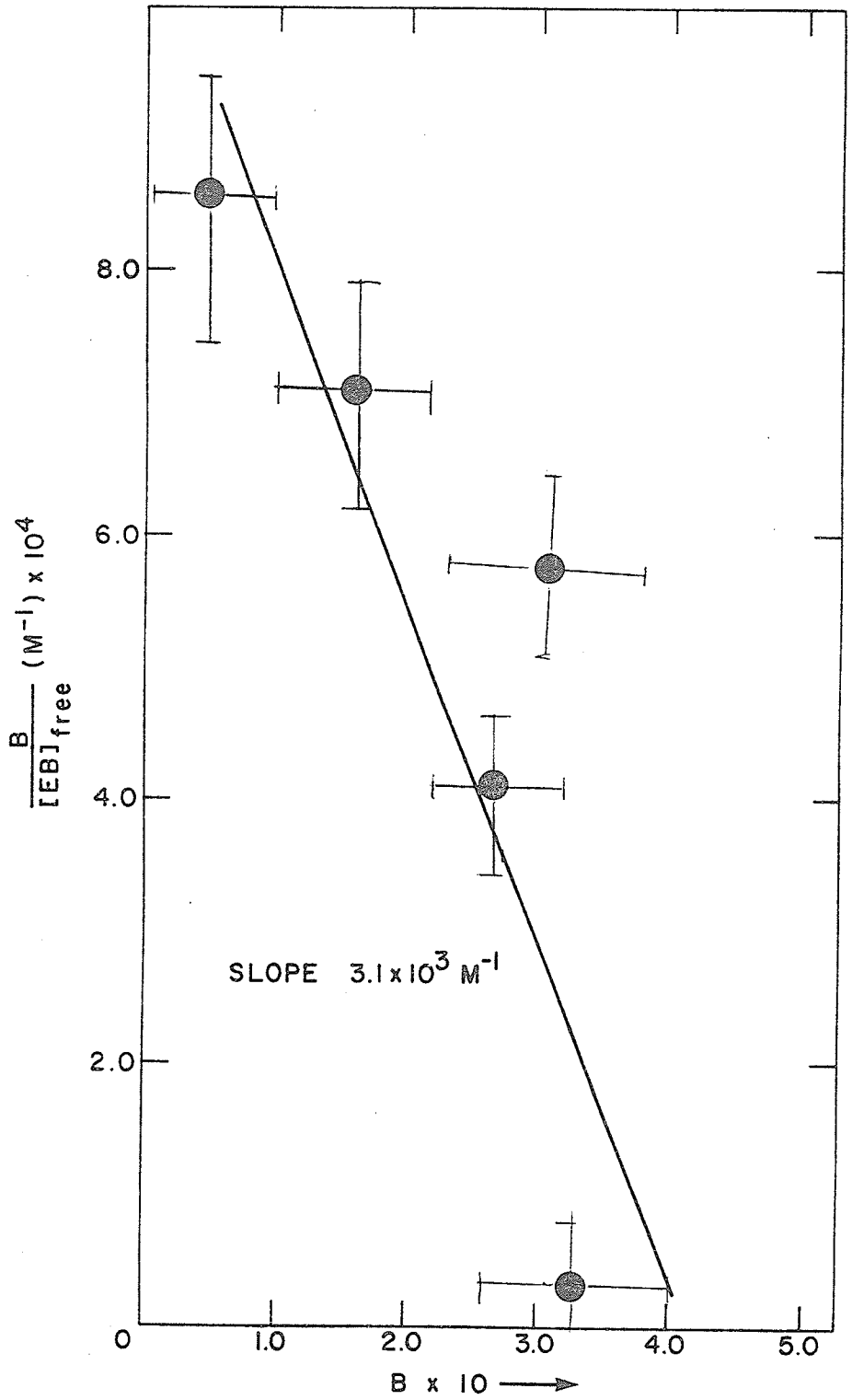

Figure 13: A Scatchard type plot for the binding of EB to Poly U. Lack of secondary structure in the Poly U molecules results in one class of binding site.

Due to the number of peaks and overlapping of peaks, analysis of NMR spectra of polynucleotides is complex and time consuming. It is limited to the simpler molecules and has not so far led to useful results which confirm or deny our present interpretation of Figs. 12 and 13.

c) Interaction of Radiation Modifiers and DNA

The pulse radiolysis method has been used to screen radiation sensitizers and radiation protectors with respect to their specificity for binding to different biopolymers (20,41). DNA is considered to be a critical target for radiation induced cell killing. The mechanism of radiosensitization by electron affinic compounds, and radioprotection by -SH compounds appears to be by free radical scavenging, or interaction with potentially damaged free radicals or damaged sites on important biopolymers. There may also be interference with cellular repair mechanisms. If the radiosensitizer or radioprotector is closely associated with the target molecule, its action may be more efficient.

Cysteamine which is a reducing agent has radioprotective properties. The decrease in e^-_{aq} reactivity on the addition of DNA to a solution of cysteamine indicates some measure of cysteamine - DNA molecular association (Table 4). This association may have important implications in cellular radioprotection. The e^-_{aq} rate constant found when DNA was added to cysteamine was corrected for the e^-_{aq} lifetime in a system containing only DNA. The decrease in e^-_{aq} reactivity on the addition of DNA to cysteamine is not dramatic, indicating that there is not complete molecular association, even at the cysteamine concentration of 10^{-4}M. When the cysteamine concentration is doubled some cysteamine

Table 4

e^-_{aq} Reaction Rate Constants with Radiation Modifiers and Macromolecules

Solution Components	$k_{e^-_{aq}}$ ($\times 10^{10}$ M^{-1} s^{-1})
Cysteamine 10^{-4}M	2.2
Cysteamine 10^{-4}M + DNA .02%	1.4
Cysteamine 2×10^{-4}M	2.9
Cysteamine 2×10^{-4}M + DNA .02%	1.9
Dehydroascorbate 10^{-4}M	1.8
Dehydroascorbate 10^{-4}M + DNA .02%	0.3
Dehydroascorbate 10^{-4}M + Chondroitin sulphate .02%	0.1
Dehydroascorbate 10^{-4}M + Myoglobin .02%	1.1

is probably free in solution as the reaction rate increases to $1.9 \times 10^{10} M^{-1} s^{-1}$. However, some association is evident and this association may have important implications in cellular radioprotection.

Dehydroascorbate, a strong oxidant and radiosensitizer, was screened for potential binding to DNA. e^-_{aq} decay rates indicate binding of dehydroascorbate to both DNA and chondroitin sulphate. When dehydroascorbate was combined with myoglobin there was a small decrease in e^-_{aq} reactivity. This indicates that the association is probably electrostatic in nature, since myoglobin is a neutral molecule while both DNA and chondroitin sulphate are anions. (These results are shown in Table 4).

N-ethymaleimide (NEM) showed little affinity for binding DNA and is known to react with -SH groups. This -SH inhibition is believed to be the probable mechanism of its biological action.

Pulse Radiolysis is a convenient , simple and useful method of screening potential DNA modifiers.

d) Interaction of Paraquat and DNA

The herbicide paraquat, or 1, 1' -dimethyl -4,4'-bipyridylium ion, was screened for its possible association with DNA, by pulse radiolysis (20). At the concentration tested (5×10^{-4} M paraquat with 0.1% DNA) there was strong association. Since the commercial use of paraquat in 1962 as a herbicide, it has proved to be highly toxic when ingested or absorbed through cutaneous lesions (70), with unusual pulmonary specificity. The underlying mechanisms of its toxicity are still incompletely understood. Evidence indicates (71) that paraquat undergoes redox cycling, with the sequential production of superoxide radicals and singlet oxygen, which initiates membrane lipid peroxidation. The effects are exacerbated by the presence of oxygen. The physiological results of this are pulmonary damage, decreased metabolic activity and enzyme inhibition.

The structure of paraquat (shown below), with its cationic charge and flat aromatic ring structure resembles that of several intercalative drugs with pharmacological properties. It seems possible, therefore, that intercalation and electrostatic attraction may take place in the binding of paraquat to DNA.

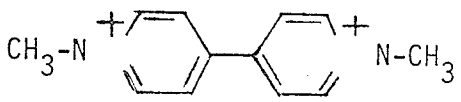

Paraquat

Paraquat concentrations were increased from 10^{-4} M to 4×10^{-4} M and the DNA concentration was kept constant at 0.02%. Decrease in e^-_{aq} reactivity on the addition of DNA to paraquat as shown in figure 14 is evidence of binding of paraquat to DNA.

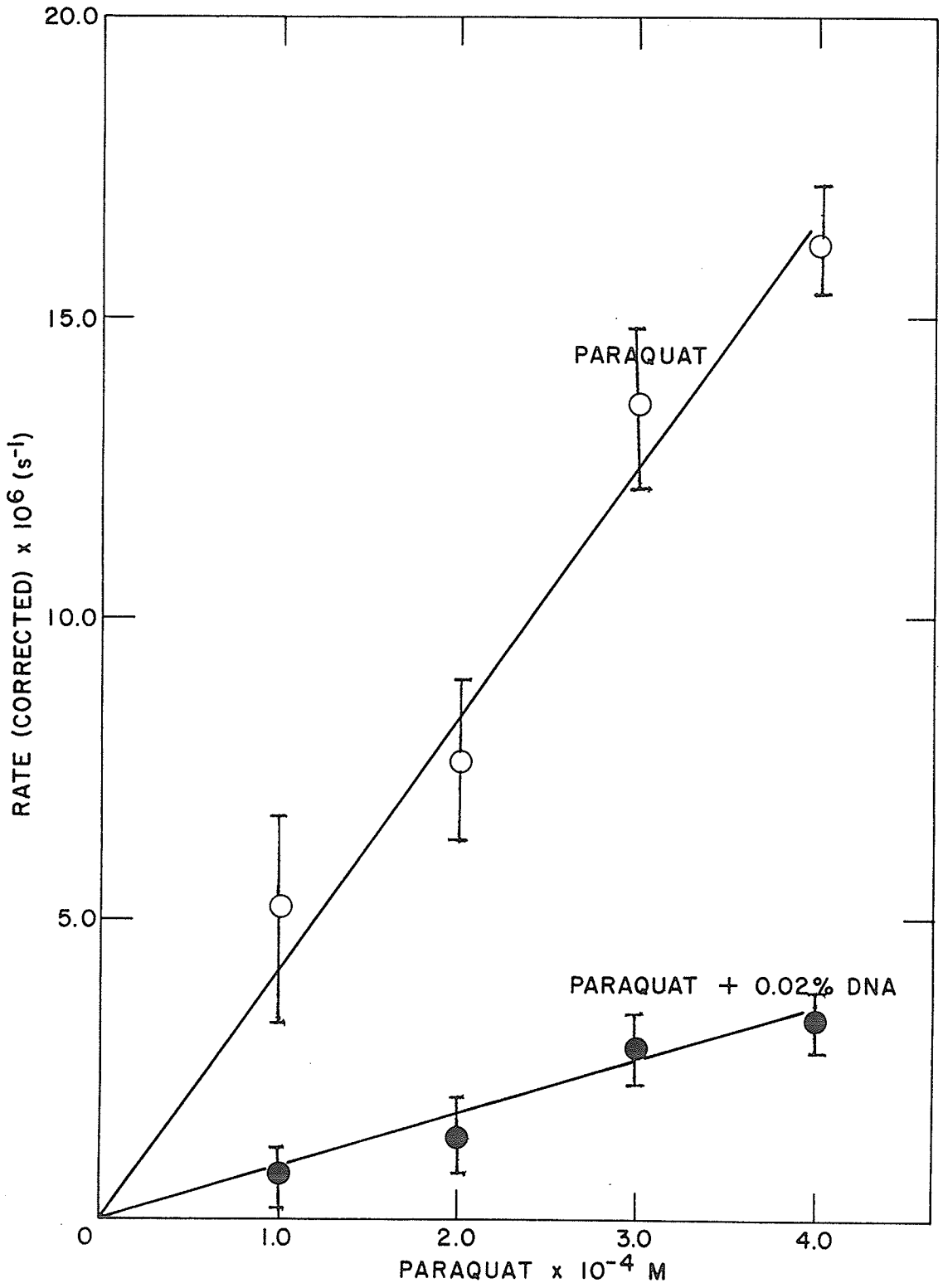

Figure 14: The rate of decay of e^-_{aq} absorption with increasing concentration of paraquat. Addition of DNA results in a decrease in e^-_{aq} reactivity due to complex formation of paraquat with DNA.

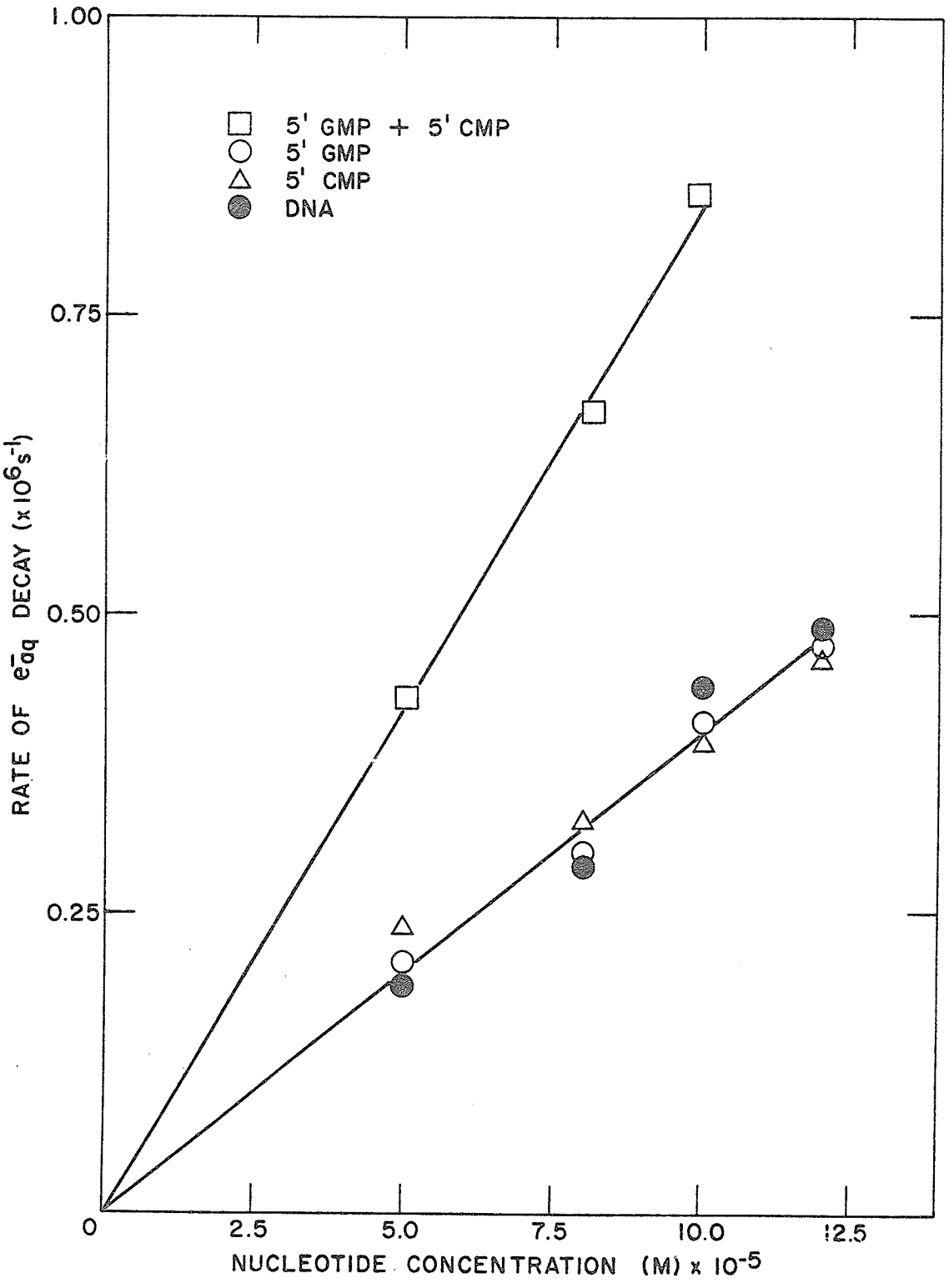

Figure 15: The rate of decay of e^-_{aq} absorption in the presence of mononucleotides and DNA. If mononucleotides associate, their decay rate will approach that of DNA for equal concentrations of mononucleotides and DNA.

e) Molecular Self-Association

The pulse radiolysis method was used in an attempt to study possible stacking interactions of ribonucleoside-5'-monophosphates. Other techniques have not revealed any evidence of stacking of these molecules in dilute solution. Results obtained by these preliminary experiments are tentative and unconfirmed. They do not prove that molecular self-association takes place. Further experiments will have to be conducted before any firm conclusions can be reached.

Ribonucleoside-5'-monophosphates, being much smaller molecules than nucleic acids will, if freely dispersed, exhibit greater molecular mobility than the polynucleotides in aqueous solution. The e^-_{aq} reactivity in such a solution should therefore be greater than in a DNA solution containing an equal concentration of nucleotides. If 5'-ribonucleotides self-associate by hydrogen bonding and vertical stacking, or are prevented from freely diffusing by self-induced changes in the solution upon dissolving, such as the microviscosity or the water structure, they will become less mobile and will behave effectively as macromolecules. Any such changes in solute mobility will be reflected, by the pulse radiolysis assay, in a reduction in the e^-_{aq} reactivity of the solute, analogous to that observed for polynucleotides and other macromolecules.

A few experiments of a preliminary nature were performed in order to look for such effects, and equal concentrations of DNA, 5'-CMP and 5'-GMP were used. The concentrations were 5×10^{-5}M, 8×10^{-5}M, 10^{-4}M and 1.2×10^{-4}M. The e^-_{aq} rate of decay was measured in solutions containing each of these molecules in turn, at the concentrations specified. Equal quantities of 5'-GMP and 5'-CMP were then put together and the total e^-_{aq} rate of decay determined. Results of the first experiment are shown in figure 15. There is an increase in e^-_{aq} decay rate with increasing concentration of all three substances. This is to be expected. However, the e^-_{aq} decay rates for equal concentrations of nucleotides appear to be comparable to those for DNA, even though each nucleotide monophosphate molecule is considerably smaller than a DNA polymer. For purposes of comparison, the e^-_{aq} decay rate in the presence of ethidium bromide is shown below in Table 5. EB is a small molecule (molecular weight = 394) without a great tendency to aggregate.

Table 5

e^-_{aq} Decay Rates with Increasing Concentrations of EB

EB concentration	e^-_{aq} decay rate ($\times 10^6$) s^{-1}
5×10^{-5} M	2.04
8×10^{-5} M	3.2
10^{-4} M	4.3
1.2×10^{-4} M	5.2

On combining equal concentrations of 5' - GMP and 5' - CMP, the e^-_{aq} rates of decay are doubled as expected. The decay rates for mixtures of 5' - GMP and 5' - CMP are comparable with equivalent concentrations of DNA. The e^-_{aq} decay rate for equimolar concentrations of 5' - GMP and 5' - CMP (5×10^{-5} M) and for 10^{-4} M DNA is 0.44×10^6 s^{-1}. The trend appears to continue with higher concentrations. 5'- GMP and 5'-CMP do not appear to be antagonistic or to inhibit each other from the effects resulting in an apparent lower mobility. The mixture of monophosphates behaves from the kinetic point of view, like the DNA biopolymer, with respect to e^-_{aq} reactivity. This is possibly because stacked molecules of 5'-GMP tend to associate with stacked molecules of 5'-CMP (74), forming an effective biopolymer. However, this is only one possible explanation of these tentative results, and such an hypothesis remains to be evaluated and tested by further experiments. Another possible interpretation of the data, is based on the premise that the repeating nucleotide subunits in a polymer are exposed and unshielded (unlike bound drugs and dyes which may be buried) and are "seen" by any diffusing reactive e^-_{aq} with approximately the same reaction cross-section. By this model, the overall e^-_{aq} reactivity of a nucleic acid, which is determined principally by its low mobility, in agreement with the Debye equation for diffusion controlled reactions, will be low. However, for individual subunits, although the probability of interaction with e^-_{aq} is reduced by their non-uniform spacial

distribution, nevertheless, for those reactants that do ultimately collide, the reactivity which is determined by reaction cross-section will be similar to that of free nucleotides.

It must be pointed out that these experiments are preliminary, and have not been repeated or confirmed by additional experiments. At present, we can make no firm conclusions on the basis of a single experiment. It appears, however, that these tentative results are consistent with the hypothesis that mononucleotides in dilute solution may interact in some way to produce an anomolous low mobility, and that the e^-_{aq} decay rate may be used as a measure of this "self-association" or "freezing" of mononucleotides. Mononucleotides may associate in aqueous solution by hydrogen bonding to water molecules, and stacking, the planar bases and nucleotides stacking on top of each other by short range forces. There is NMR evidence to support this (74) for concentrated solutions ($\geq 10^{-2}$M), but this experiment is the first report to suggest a similar effect may occur in dilute solutions. Further experiments to verify these results will have to be done in order to establish a firm experimental basis for such an hypothesis. By NMR, upfield spectral shifts of ring protons are observed when there is stacking of aromatic bases. Hydrogen bonding results in downfield peak shifts for the participating protons. In the case of GMP, AMP and to a lesser extent CMP, pronounced upfield shifts were observed for the ring protons and H-1' proton, at high concentrations ($\geq 10^{-2}$M), indicative of stacking interactions (74). Possible base stacking in the pyrimidine nucleosides (cytidine and uridine) cannot be observed by NMR because of the absence of ring currents, but, based on experiments with other

mononucleotides, none is expected at dilute concentrations.

If the results in figure 15 can be confirmed by additional pulse radiolysis experiments, then they are very interesting and may indicate a new application of the pulse radiolysis assay, in which e^-_{aq} reactivity may be used to estimate subtle interactions in small molecules like mononucleotides, not detectable by other means.

f) Macromolecular Association

Histones are essential for the structure of chromosomes in the nuclei of eukaryotic cells. They have a great affinity for DNA and a fairly high molecular weight (~10,000). They stabilize DNA in the duplex state, and are species specific, even though arginine-rich histones are markedly similar in different tissues and in widely different species.

In order to determine if the association of molecules with a high molecular weight could be detected by this method, histones ranging in concentration from 0.01% to 0.05% were added to 0.01% DNA and 0.02% DNA. There was a reduction in e^-_{aq} reactivity as shown in figure 16, indicating considerable association of histone and DNA.

Because of their basic nature, histones can neutralize the phosphate groups of DNA, thus contributing to its organization in the double helical form. X-ray and biochemical analyses (75) suggest that tightly packed regions of coiled DNA and associated protein alternate with more extended DNA like a string of beads. The extended regions are then available for enzymatic cleavage.

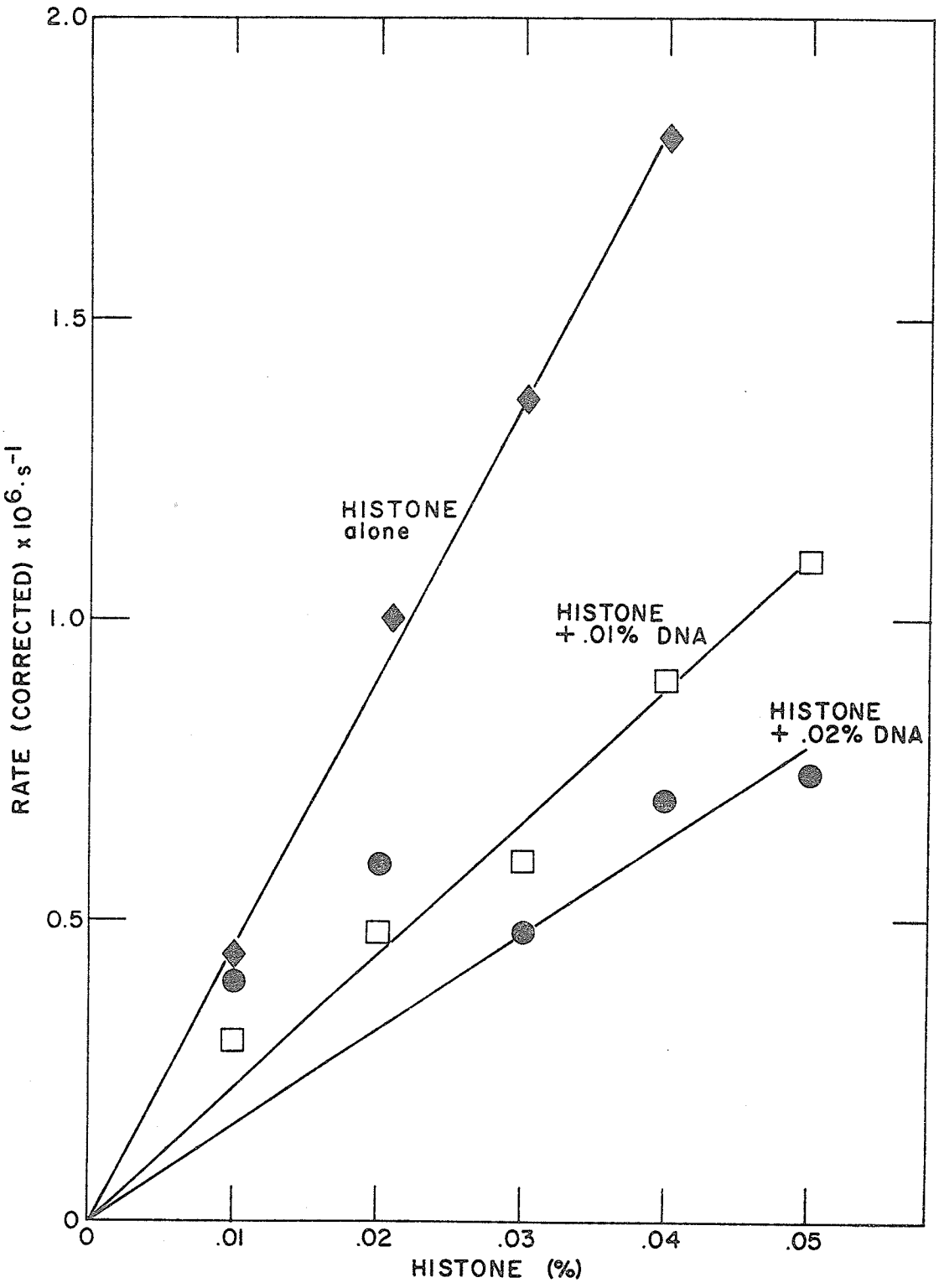

Figure 16: The effect of adding increasing concentrations of DNA to histones, on the rate of decay of e^-_{aq} absorption at 650 nm. The rate decreases with increasing DNA concentration, as there are more binding sites for histones.

Chapter V

CONCLUSIONS

The pulse radiolysis method has the potential of being an indispensable tool in the study of molecular interactions. Binding parameters obtained for the association of acridine orange and DNA using this method are in close agreement with results obtained by conventional techniques. The Scatchard-type plot showed two classes of bindings sites, one due to energetically strong and the other due to energetically weak binding of AO to DNA. Association constants obtained were $8 \times 10^5\ M^{-1}$ and $5 \times 10^3\ M^{-1}$, respectively, for strong and weak binding, and the ratios of bound dye to biopolymer subunit were 0.1 and ~ 1.0, respectively. Association constants obtained by conventional methods are $\sim 2 \times 10^5\ M^{-1}$ and $4 \times 10^3\ M^{-1}$, respectively, and the ratio of bound dye to nucleotide subunit is ~ 0.1 for saturation of the strong complex, ~ 1.0 for saturation of the weak complex. Numerous mutagens, carcinogens, antibiotics and antitumour agents such as aminoacridines, benzacridines, actinomycins, phenanthridines etc. have a similar planar ring structure to AO. Intercalation may be a common mode of strong interaction of these drugs with DNA, particularly when they are cationic. The electrostatic nature of the binding was also established by combining AO with the anionic macromolecules chondroitin sulphate and myoglobin, with positive results. There was no association with the essentially neutral molecules of bovine serum albumin.

Inaccuracies can arise when using this method because of the high rate of reactivity of e^-_{aq} with impurities, including oxygen and the products of radiolysis of water. All traces of oxygen and ·OH radicals must be removed, but hydrated electrons will still react with each other. This leads to greater errors when the concentration of solute is very low. There is a limit to the use of the

method. For instance, in the limiting case of extremely strong binding ($K \sim 10^6 M^{-1}$) of small molecules to polymers, the technique is limited, in terms of accurate and precise determination of e^-_{aq} reactivity, to the analysis of micromolar quantities of solute. This is quite comparable with the sensitivity of other conventional spectroscopic techniques.

In probing other applications of this method it was found that molecular conformational changes also can be detected, not only structural changes that result in the shielding of electron-affinic sites on the macromolecule which has relevance in the study of radiosensitization. The strong binding of ethidium bromide was diminished on association with denatured DNA, the number of sites for intercalation being reduced. Reduced association was also observed with mononucleotides. It has, therefore, been established that pulse radiolysis is a useful tool in studying structural changes in polynucleotides, by monitoring the association of a known intercalant. The manner in which the structural change occurs does not affect the results, making this a potential tool in investigating radiation damage to polynucleotides and other macromolecules.

Molecular associations may also be observable, as inferred from tentative observations with mononucleotides. In one experiment, the e^-_{aq} rate of decay with nucleotide monophosphates has been found to be the same as that obtained with an equal effective concentration of DNA nucleotides. In the latter case a biopolymer is present, suggesting that in the former, the nucleotides may be behaving in an analogous manner to solutes associated with or incorporated in macromolecules. There was also a marked decrease in e^-_{aq} reactivity when histones were combined with DNA. The pulse radiolysis method can therefore be used to investigate the association of both small and large molecules.

The role of pulse radiolysis in the screening of potentially toxic drugs is seen in the interaction of paraquat and DNA. The toxic herbicide accumulates in mammalian organs, particularly the lungs where membrane lipid peroxidation occurs. The mechanism of action has not been fully elucidated but it appears that its interaction with DNA may play a role in its toxicity.

Radioprotectors and radiosensitizers if bound to DNA, the primary cellular target of radical attack, should act more efficiently. The radioprotector cysteamine was found to bind to DNA. At the same time, experimental evidence has shown that cysteamine protects by attacking endonucleases. The interaction of cysteamine and DNA in the presence of endonuclease may be as important in radioprotection as the scavenging of free radicals by cysteamine. The radiosensitizer NEM did not bind DNA, but dehydroascorbate associated with DNA. The electrostatic nature of the binding was investigated and confirmed by combining dehydroascorbate with chondroitin sulphate and myoglobin, with positive results. Thus pulse radiolysis is also a method of investigating the action of radiation modifiers.

Pulse radiolysis is very useful in studying molecular interactions and associations, can be used to screen potentially harmful drugs, and to investigate the action of chemical modifiers of radiation damage to cell constituents.

Pulse radiolysis, like NMR and other analytical techniques, is a static method and does not provide direct evidence for binding mechanisms. It provides information on binding parameters and the strength and extent of binding. The factors that affect binding such as pH, temperature and ionic strength may also be studied. The probable cause of binding is inferred from this data. The information is obtained simply and rapidly, without perturbing the system or requiring the molecules to have specific properties.

Pulse radiolysis is probably unique in its universality and versatility. Other methods such as NMR are complicated, time-consuming and limited to specific molecules, but complement the Pulse Radiolysis method because they provide information on the electronic configuration and atomic structure of complexes.

Pulse Radiolysis has great potential in drug screening and in the research and development of new drugs by analogy with known macromolecular modifiers. The scope and potential of the method appear to be great.

REFERENCES

1. Pullman, B., ed. Molecular Associations in Biology, Academic Press (1968).

2. Ariens, E.J., ed. Physico-chemical Aspects of Drug Action, Pergamon Press (1968).

3. Knock, F.E. Anticancer agents, Charles C. Thomas Publ. (1967).

4. Anton, A.H. and Solomon, H.M., eds. Annals. New York Acad. Sci. Vol. 226 (1973).

5. Lerman, L.S. J. Cell. and Comp. Physiol., 64: Suppl. no. 1-18 (1964).

6. Goldstein, A., Aronow, L. and Kalman, S.M. eds. Principles of Drug Action. J. Wiley & Sons (1968).

7. Breccia, A., Rimondi, C. and Adams, G.E., eds. Radiosensitizers of Hypoxic Cells (1979).

8. Adams, G.E., Fowler, G.E. and Wardman, P., eds. Brit. J. Cancer. suppl. No. III June 1978.

9. Greenstock, C.L., Ng, M. and Hunt, J.W., Advances in Chemistry Series, No. 81, 397-417 (1968).

10. Debye, P., Trans. Electrochem. Soc. 82, 265 (1942).

11. Ebert, M., Keene, J.P. and Swallow, A.J. eds., Pulse Radiolysis, Academic Press (1969).

12. Matheson, M.S. and Dorfman, L.M., eds. Pulse Radiolysis, The M.I.T. Press (1969).

13. Hart, E.J. and Anbar, M. eds., The Hydrated Electron, J. Wiley & Sons (1970).

14. Phillips, G.O., Power, D.M., Robinson, C. and Davies, J.V. Biochem. Biophys. Acta, 295, 8-17 (1973).

15. Greenstock, C.L. and Ruddock, G.W. Chem., Biol. Interactions, 11, 441-447 (1975).

16. Phillips, G.O., Power, D.M., Robinson, C., and Davies, J.V. Biochem Biophys. Acta, 215, 491-502 (1970).

17. Phillips, G.O., Power, D.M. and Richards, J.T. Israel J. Chem. 11, No. 4, 517-527 (1973).

18. Wainwright, P., Power, D.M. and Thomas, E.W. Int. J. Radiat. Biol. 33, No. 2, 151-162 (1978).

19. Chaudhuri, S., Phillips, G.O., Power, D.M. and Davies, J.V., Int. J. Radiat. Biol. 28, No. 4, 345-352 (1975).

20. Greenstock, C.L. and Ruddock, G.W., Biochem. Biophys. Acta, 383, 464-467 (1975).

21. Waring, M.J., J. Mol. Biol. 13, 269-282 (1965).

22. LePecq, J.B. and Paoletti, C.J. Mol. Biol. 27, 87-106 (1967).

23. Blake, A. and Peacocke, A.R. Biopolymers, 6, 1225-1252 (1968).

24. Scatchard, G. Ann. N.Y. Acad. Sci., 51, 660 (1949).

25. Burns, V.W.F. Exptl. Cell Res. 75, 200-206 (1972).

26. Gafni, A., Schlessinger, J. and Steinberg, I.Z. Israel J. Chem. 11, 423-434 (1973).

27. Bittman, R. and Blau, L., Biochem. 14, 2138-2145 (1975).

28. Shin, Yong Ae. Biopolymers 12, 2459-2475 (1973).

29. Muller, W. and Crothers, D.M., J. Mol. Biol. 35, 251-290 (1968).

30. Speitor, R., Torkin, D.T. and Lorenzo, A.V., J. Pharm. Pharmacol. 24, 786 (1972).

31. Bauer, O. and Vinograd, J.J. Mol. Biol. 54, 281-298 (1970).

32. Schwarz, J.C.P. Physical Methods in Organic Chemistry, Oliver and Boyd (1964).

33. Devek, R.A. NMR in Biochemistry, Clarendon Press, Oxford (1973).

34. Bovey, Frank A. High Resolution NMR of Macromolecules. Academic Press (1972).

35. Wüthrich, Kurt. NMR in Biological Research; Peptides and Proteins. Oxford, North-Holland (1976).

36. Blears, D.J. and Danyluk, S.S. J. Am. Chem. Soc. 88, 1084 (1966).

37. Patel, Dinshaw J., Accounts of Chemical Research 12, 118-125 (1978).

38. Krugh, T.R. and Neely, J.W. Biochem. 12, 1775-1782 (1973).

39. Krugh, T.R. and Neely, J.W. Biochem. 12, 4418-4425 (1973).

40. Patel, D.J. Biochem. 13, 1476-1482 (1974).

41. Danyluk, S.S. and Victor, T.A. Jerusalem Symp. Quant. Chem. Biochem. Vol. II 394-411 (1970).

42. Brenner, S., Barnett, L., Crick, F.H.C. and Orgel, A., J. Mol. Biol. 3, 121 (1961).

43. Lerman, L.S., J. Mol. Biol. 3, 18 (1961).

44. Spinks, J.W.T. and Woods, R.J. eds., An Introduction to Radiation Chemistry, J. Wiley and Sons (1976).

45. Platzman, R.L. Radiat. Res. 2, 1 (1955).

46. Draganic, I.G. and Draganic, Z.N., The Radiation Chemistry of Water, Academic Press, New York, 1971.

47. Hunt, J.W., Greenstock, C.L. and Bronskill, M.J. Int. J. Radiat. Phys. Chem. 4, 87-105 (1972)

48. Simic, M., Neta, P. and Hayon, O.E. J. Phys. Chem. 73, 3794 (1969).

49 Lopata, V.J., Dunlop, I.H., Greenstock, C.L. and Dixon, R.S. Pulser-A Computer program for kinetic analysis of pulse radiolysis and flash photolysis data, Whiteshell Nuclear Research Establishment Report, WNRE-276 (1975).

50. Greenstock, C.L., Banerjee, C. and Ruddock, G.W. Fourth Symposium on Radiation Chemistry, Adademiai Kiado, Budapest, 871-879 (1976).

51. Buchanan, J.D., Power, D.M., Phillips, G.O. and Davies, J.V. Int. J. Radiat. Biol. 33 (6), 551-562 (1978).

52. Peacocke, A.R. Acridines. Interscience Publ.

53. Boyle, R.E., Nelson, S.S., Dollish, F.R. and Olsen, M.J. Arch. Biochem. Biophys. 96, 47-50 (1962).

54. Zanken, V. Physik Chem. 199, 225 (1952).

55. Hruska, F.E. and Danyluk, S.S. Biochem. Biophys. Acta, 161, 250-252 (1968).

56. Lerman, L.S. J. Mol. Biol. 10, 367 (1964).

57. Peacocke, A.R. and Skerett, J.N.H. Trans. Far. Soc. 52, 261(1956).

58. Drummond, D.S., Simpson-Gildemeister, V.F.W. and Peacocke, A.R. Biopolymers, 3, 135(1965).

59. Ficks, Z. and Smith, K.C., Radiat. Res. 48, 63-73 (1971).

60. Chambron, J., Daune, M. and Sadron, C. Biochem. Biophys. Acta 123, 306 (1966).

61. Gilbert, M. and Claverie, P., J. Theor. Biol. 18, 330 (1968).

62. Ichimura, S., Zama, M., Fryita, H. and Ito, T. Biochem. Biophys. Acta 190, 116 (1969).

63. Braams, R. and Ebert, M. Adv. in Chem. Series No. 81, 464 (1968).

64. Waring, M.J. Biochem. Biophys. Acta 114, 234-244 (1966).

65. Aktipis, S. and Kindelis, A. Biochem. 12, 1213 (1973).

66. Morgan, A.R. and Pulleyblank, D.E., Biochem. Biophys. Res. Commun. 61, #2, 396-403 (1974).

67. Simpkins, H. and Richards, E.G., J. Mol. Biol. 29, 249 (1967).

68. Arnott, S., Chandrasekaran, R. and Marttila, C.M. Biochem. J. 141, 537 (1974).

69. Michelson, A.M. and Monny, C. Proc. N. A. S. 56, 1528 (1966).

70. Newhouse, M., McEvoy, D. and Rosenthal, D. Arch. Dermatol. 114 (10), 1516-1519 (1978).

71. Bus, J.S., Aust, S.D. and Gibson, J.E., First Iowa Symposium on Toxic Mechanisms. Mechanisms of Paraquat Toxicity. pp. 157-174 (1977).

72. Broom, A.D., Schweizer, M.P. and Ts'o, P.O.P. J. Am. Chem. Soc., 89, 3612 (1967).

73. Pinnavaia, T.J., Miles, H.T. and Becker, E.D., J. Am. Chem. Soc. 86, 4182 (1964).

74. Raszka, M. and Kaplan, N.O. Proc. Natl. Acad. Sci. U.S.A. 69, 2025-2029 (1972).

75. Kornberg, R.D. Science 184, 868 (1974).

5.1. Subprogram "Digitizer Translator"

Flowchart

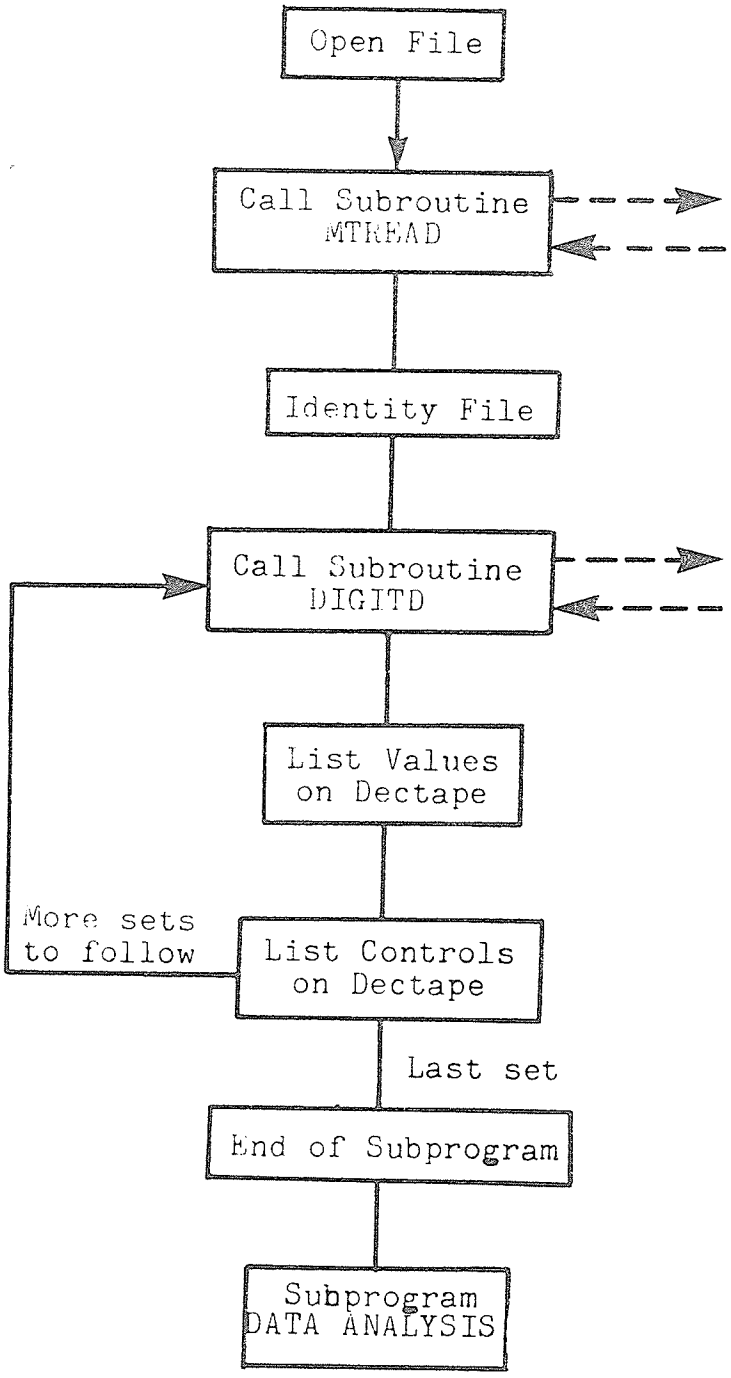

Subroutine MTREAD

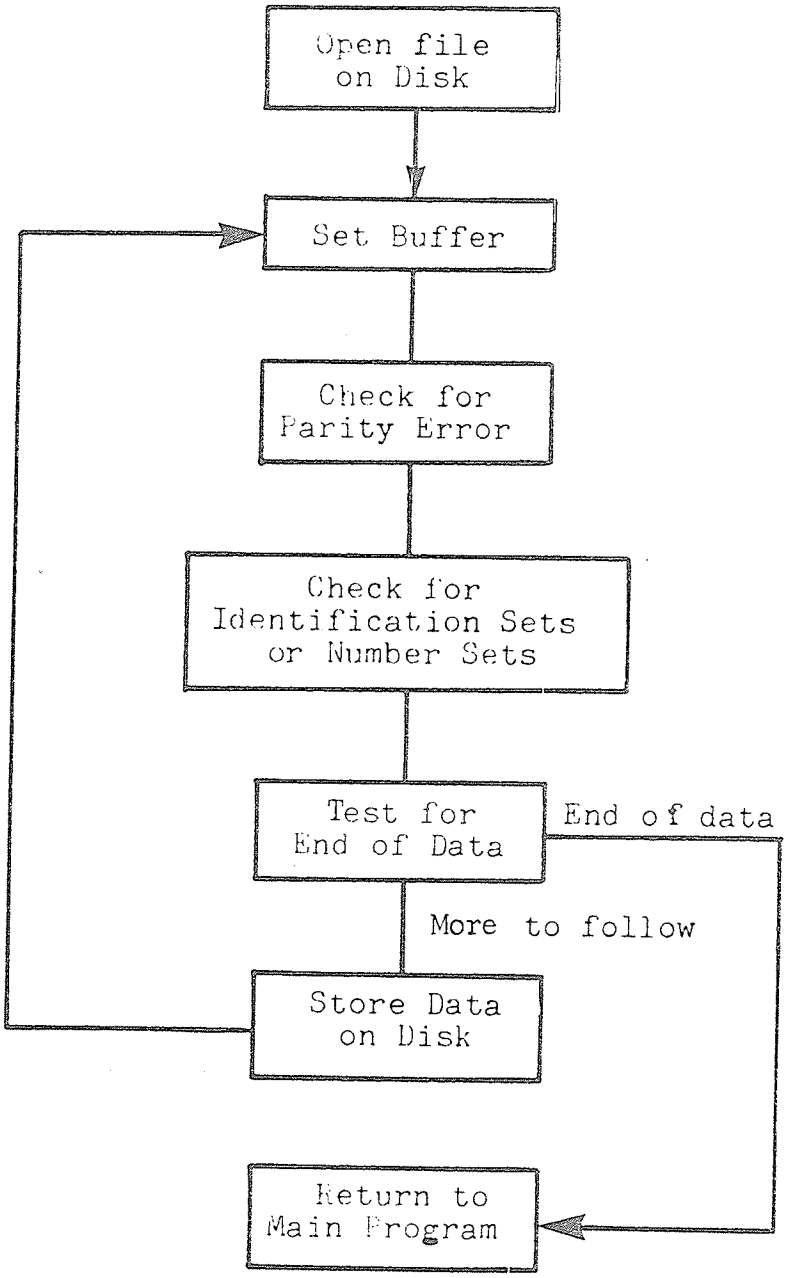

Subroutine DIGITD

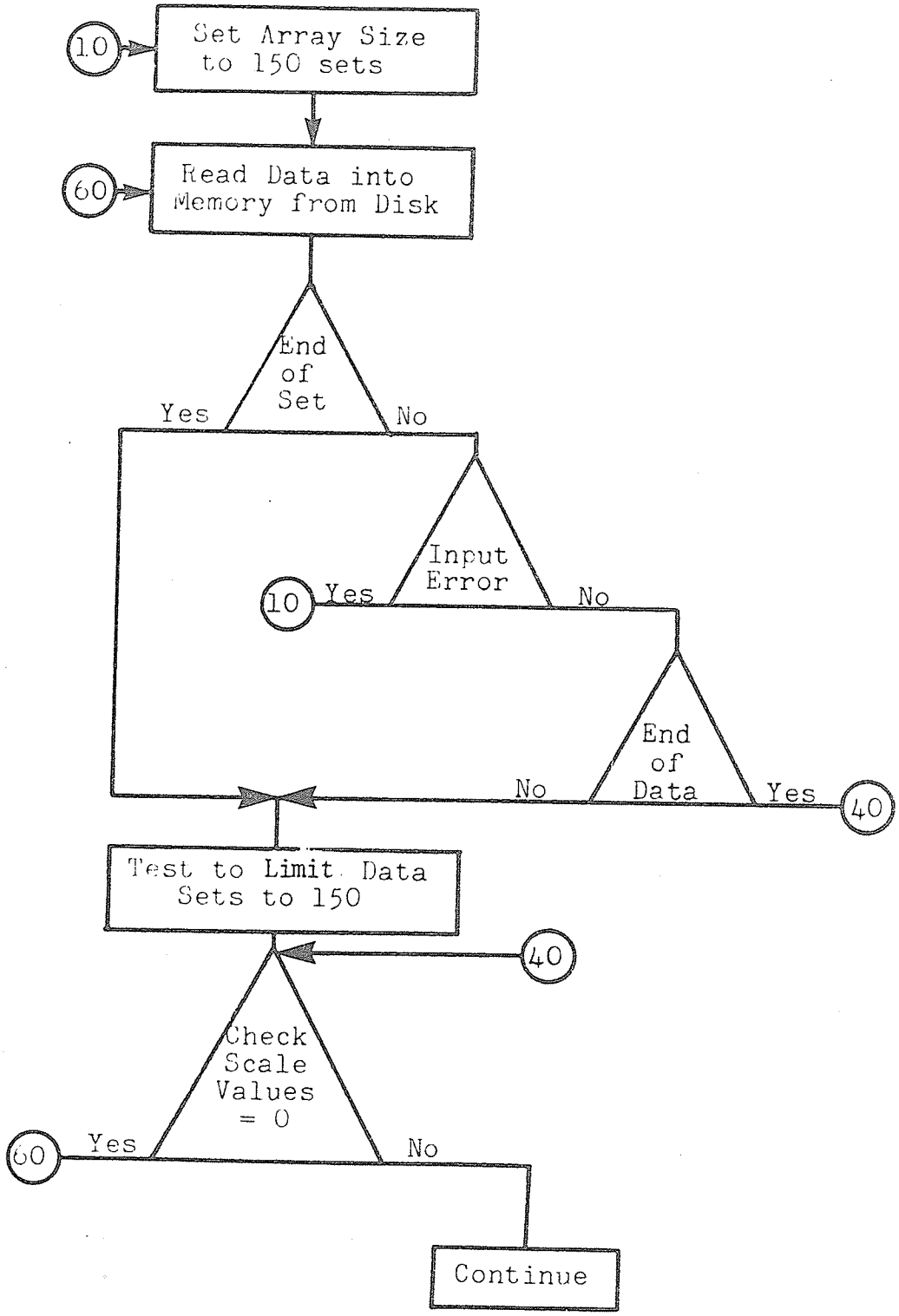

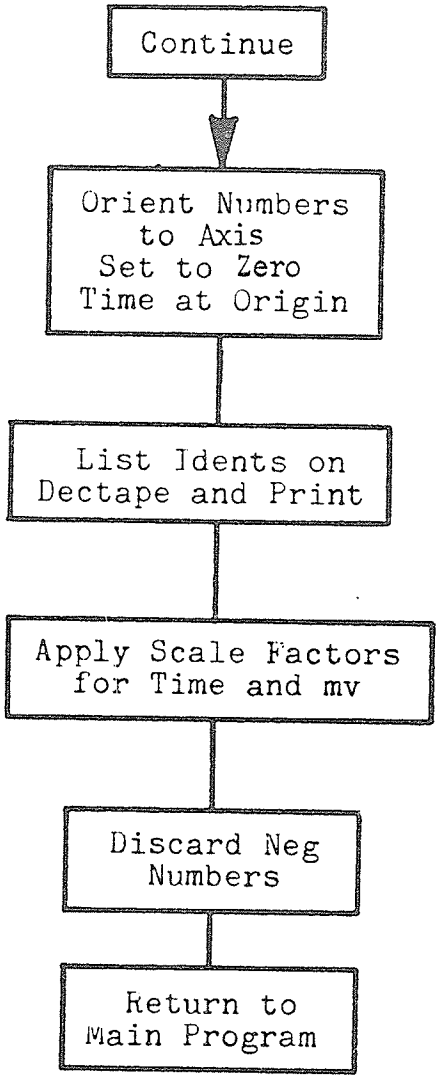
Continue
Orient Numbers to Axis Set to Zero Time at Origin
List Idents on Dectape and Print
Apply Scale Factors for Time and mv
Discard Neg Numbers
Return to Main Program

Subprogram - "Digitizer Translator"

```
C PROGRAM TO RATIONALIZE PHOTO NUMBERS FOR PULSE RAD EXP
C
      IMPLICIT DOUBLE PRECISION (A-H,O-Z)
      REAL FILNAM,DUM
      COMMON X(150),Y(150), IDENT(3),N,J,JDENT(3),NM
      COMMON    IDAT(50), MTH(50), IPHOT(50), ICASE(50), IDC(50),
     1IAC(50),IWAVE(50),IYR(50),CONC(50),TIME(50),DLEV(50),XMONT(50)
      INTEGER IDAT,MTH,IYR,IPHOT,ICASE,IDC,IAC,IWAVE
      READ 1000,OF
      READ 1000,FILNAM,INDIC
      PRINT 555,OF,FILNAM
  555 FORMAT (' FILE NAME CORRECTED DATA,'A5,/,
     C'FILE NAME RAW DATA,'A5)
 1000 FORMAT (A5,I1,4X,D10.0)
C     IF INDIC=0,PROGRAM EXPECTS DATA ON DECTAPE FILE NAMED 'FILNAM'
C     (UNIT 7)
C     IF INDIC=1,PROGRAN EXPECTS DATA ON MT. AND WILL WRITE FILE
C     NAMED FILNAM ON DISK (UNIT 7)
C
      IF (INDIC.EQ.1) CALL MTREAD (FILNAM,INDIC)
      CALL IFILE (7,FILNAM)
      CALL OFILE(8,OF)
      DO 800 NM = 1, 50
      READ (5,200,END=800) IDAT(NM),MTH(NM),IYR(NM),IPHOT(NM),IWAVE(NM),
     1CONC(NM), TIME(NM), IDC(NM), DLEV(NM), IAC(NM),ICASE(NM),
     2XMONT(NM)
  200 FORMAT (3I2,2I3  ,2E6,?  ,1I3,1F6.1,1I3  ,6X,1I1,1F5.3)
      IF(IDAT(NM).EQ.0) GO TO 3
  800 CONTINUE
  3   N=150
C
C TO PRODUCE NUMBERS FOR TIME AND MILLIVOLTS
C
      CALL DIGITO
      J = J - 4
C
C TO LIST SET OF REAL NUMBERS FOR TIME AND MILLIVOLTS ON DEC TAPE
C
      WRITE (8,225) (X(I),Y(I),I=1,J)
  225 FORMAT (1D15.4,1D14.4)
      X(I)=0.0000
      Y(I)=0.0000
      WRITE (8,225) X(I),Y(I)
      IF(N-2) 1,2,2
    1 K = 1
      WRITE (8,226) K
  226 FORMAT (I10)
      GO TO 3
    2 K = 2
      WRITE (8,226) K
       CALL EXIT
      END
```

```
      SUBROUTINE MTREAD (FILNAM,INDIC)
C ROUTINE TO READ MAGTAPE AND LIST ON DISK (UNIT 7)
C
      DIMENSION ARRAY(4)
      CALL INTMAG(0)
      REWIND 16
      CALL OFILE (7,FILNAM)
      K=1
6     CALL BUFFR (1,556,16,15,ARRAY)
      K=K+1
C
C TO CHECK FOR PARITY ERROR IF NONE EXISTS PROGRAM WILL CONTINUE
     C IF AN ERROR EXIST SUCH WILL BE PRINTED OUT AND
     C THE PROGRAM WILL CONTINUE
C
      IF (IEND16(0)) 1,2,3
3     PRINT 100 ,K
100   FORMAT (36H PARITY ERROR ENCOUNTERED READING MT ,
     111H RECORD NO. ,I5)
      GO TO 2
1     END FILE 7
      CALL IFILE (7,FILNAM)
      J=1
7     READ (7,102,END=251)(ARRAY(I),I=1,3)
      J=J+1
      GO TO 7
104   FORMAT (1X,I10,5X,2A5,A2)
251   CONTINUE
      RETURN
2     CONTINUE
      IF (ARRAY(3)=5H     )4,5,4
5     WRITE (7,101) ARRAY(1),ARRAY(2)
101   FORMAT (A5,A3)
      GO TO 8
4     WRITE (7,102) (ARRAY (I),I=1,3)
102   FORMAT (2A5,A2)
C READS 12 CHARACTERS ALL TOGETHER
    8 IF (ARRAY(1)=5H99   ) 6,1,6
      RETURN
      END
```

```
      SUBROUTINE DIGITD
C ROUTINE TO READ POINTS FROM DISK PREPARED BY SUBROUTINE MTREAD
C AND TRANSLATE THE VALUES TO ORIGIN OF PHOTO OUTPUT
C IS THE SCALED VALUES  OF TIME ,SEC. AND MILLIVOLTS
C
      IMPLICIT DOUBLE PRECISION (A-H,O-Z)
      COMMON X(150),Y(150), IDENT(3),N,J,JDENT(3),NM
      COMMON    IDAT(50), MTH(50), IPHOT(50), ICASE(50), IDC(50),
     1IAC(50),IWAVE(50),IYR(50),CONC(50),TIME(50),DLEV(50),XMONT(50)
      INTEGER IDAT,MTH,IYR,IPHOT,ICASE,IDC,IAC,IWAVE
C
      NN=150
C      TO CHANGE DIMENSIONED SIZE OF X AND Y ARRAYS,CHANGE DIMENSION STATEME
C      AND NN
C
C     ON OUTPUT N = 0 IFTEST WAS SMALLER THAN SIZE ALLOTTED AND THIS IS
C     NOT THE LAST TEST OF THE SERIES - NORMAL RUN,
C     N = 1 IF THE SET WAS LONGER THAN THE DIMENSIONED SIZE OF THE
C     ARRAY - ONLY THE FIRST NN POINTS WILL BE USED
C     N = 2 FOR LAST TEST OF SERIES,
C     N = 3 FOR TEST TOO LONG AND LAST TEST OF SERIES,
C
C
C READ VARIABLES INTO MEMORY
C
10    N=0
   60 READ (7,105, END=250)  NUM
  105 FORMAT (I5)
C
      DO 600 K=1,NM
      IF(NUM.EQ.IPHOT(K)) GO TO 700
      IF (IPHOT(K).EQ.0) GO TO 700
  600 CONTINUE
  700 MN = K
      J=0
C
C BEGIN DIGITIZER NUMBER PROCESSING
C     READ X,Y POINT PAIRS
      DO 1 I=1,NN
      J=J+1
      READ (7,101)  X(J),Y(J)
101   FORMAT (2F4.0)
      IF (X(J).LT.8999) GO TO 1
      IF (X(J).GT.9988) GO TO 10
      IF (X(J).GT.9898) N=N+2
      GO TO 40
1     CONTINUE
C
C TEST TO ALLOW PROGRAM TO SKIP EXCESS POINTS IF THEY EXIST
C
```

```
      N=N+1
      DO 3 I=1,10000
      READ (7,101)TEST,DUM
      IF (TEST.LT.8999)  GO TO 3
      IF (TEST.GT.9989)  GO TO 10
      IF (TEST.GT.9898) N=N+2
      GO TO 40
    3 CONTINUE
C
   40 IF (TIME(MN).EQ.0.D0) GO TO 60
C
C     J=NO. OF X,Y PAIRS
C
      J=J-1
C
C ROTATION AND TRANSLATION OF AXIS
C
      THETA=DATAN2(Y(2)-Y(1),X(2)-X(1))
      ACOS=DCOS(THETA)
      ASIN=DSIN(THETA)
      DO 20 I=2,J
      XADJ=X(I)-X(1)
      YADJ=Y(I)-Y(1)
      AX=XADJ*ACOS+YADJ*ASIN
      AY=-XADJ*ASIN+YADJ*ACOS
      X(I)=AX
   20 Y(I)=AY
C
C - TO ORIENT THE X AND Y AXIS OF A PHOTOGRAPH TRACE
C
       X(1) = 0.0
      Y(1) = 0.0
      XK=X(4)-X(1)
      YK=Y(4)-Y(1)
      DO 30 I=5,J
      X(I)=X(I)-XK
      IF(Y(5).LT.YK) GO TO 70
      Y(I) = Y(I) - YK
      GO TO 30
   70 Y(I) = YK - Y(I)
   30 CONTINUE
      X(1)=0.0
      Y(1)=0.0
C
C DIGIT NUMBERS CORRECTED TO GRAPH AXIS IN MILLIMETERS
C
      XX = X(2) - X(1)
      YY = Y(3) - Y(1)
      L=0
      DO 50 K=6,J
      L=L+1
```

```
C
C REAL NUMBERS FOR AMPLITUDE AND TIME CALCULATIONS BY APPLYING SCALE
      C FACTORS OF TIME AND MV IN SECONDS AND MILLIVOLTS
C
       X(L) = X(K)*(8.0*TIME(MN))/XX
    2Y Y(L) = Y(K)*(5.0*IAC(MN))/YY
C
C LIST DAY,MONTH,YEAR ,PHOTO NUMBER,WAVELENNGTH,CONCENTRATION
      C DC LEVEL,CASE NUMBER,XMOUNT ON DEC TAPE
C
       WRITE(8,216) IDAT(MN),MTH(MN),IYR(MN),IPHOT(MN),IWAVE(MN),
      1CONC(MN),DLEV(MN),ICASE(MN),XMONT(MN), NUM
  216 FORMAT (3I2,2I3,1E10.4,1F6.1,1I1,F5.3,I3)
C
C TO DISCARD NEGATIVE NUMBERS
C
       L=0
C
C NUMBER OF SETS OF DIGIT PAIRS
C
       I=0
     7 L=L+1
     5 I=I+1
       IF(I.EQ.J) GO TO 6
       IF (Y(I).LT.0.E0) GO TO 5
       IF (X(I).LT.0.E0) GO TO 5
       X(L)=X(I)
       Y(L)=Y(I)
       GO TO 7
     6 J = L - 2
C
C NUMBER OF SETS OF POSITIVE DIGIT PAIRS
C
C
C REAL POSITIVE NUMBER PAIRS
C
       RETURN
250    N=N+2
       RETURN
       END
```

5.2 Subprogram "Data Analysis"

Flowchart

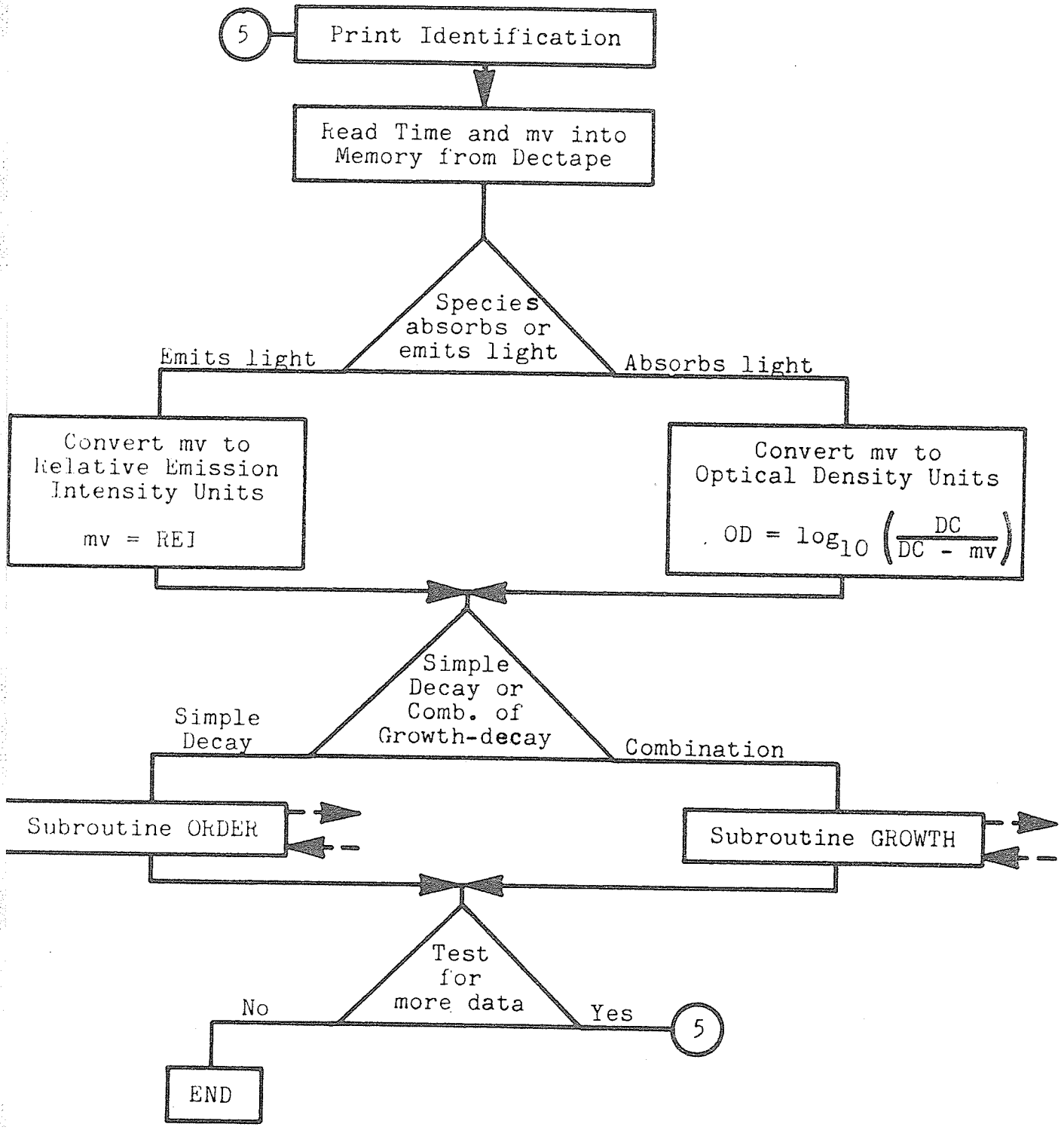

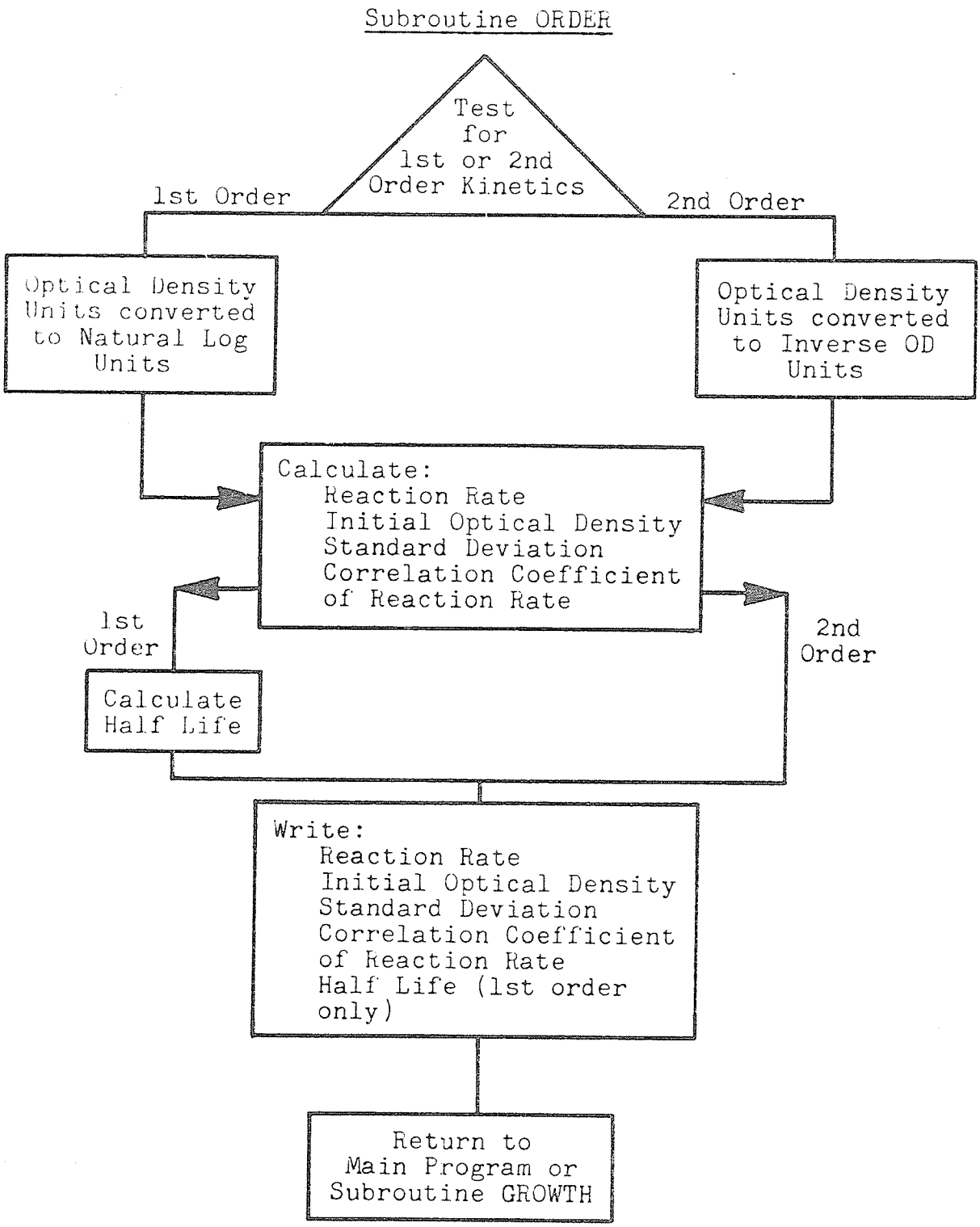
Subroutine ORDER
Test for 1st or 2nd Order Kinetics
1st Order
2nd Order
Optical Density Units converted to Natural Log Units
Optical Density Units converted to Inverse OD Units
Calculate:
Reaction Rate
Initial Optical Density
Standard Deviation
Correlation Coefficient of Reaction Rate
1st Order
2nd Order
Calculate Half Life
Write:
Reaction Rate
Initial Optical Density
Standard Deviation
Correlation Coefficient of Reaction Rate
Half Life (1st order only)
Return to Main Program or Subroutine GROWTH

Subroutine GROWTH

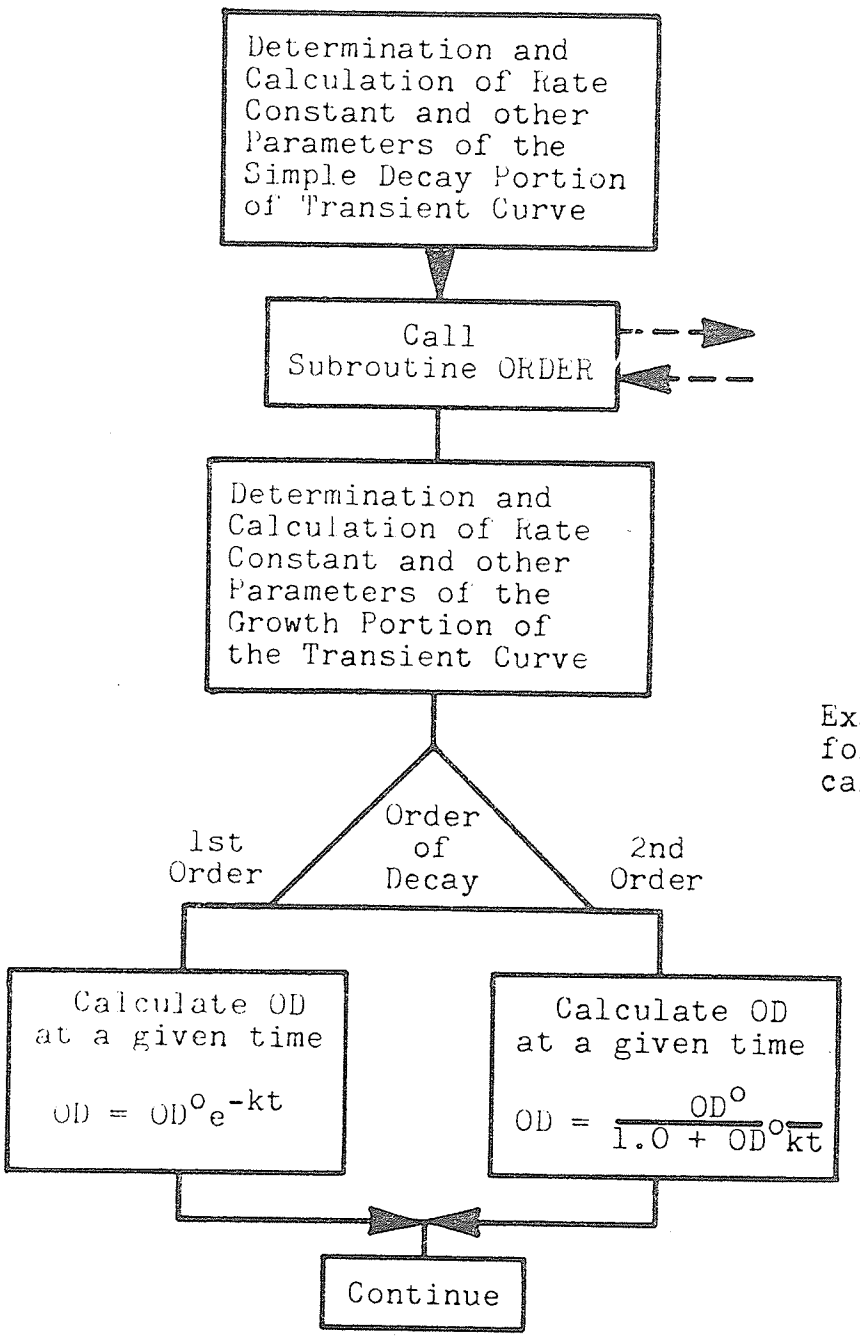

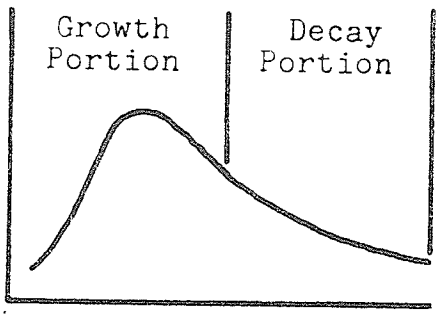

Example of Transient Signal for which subroutine GROWTH calculates the reaction rate

NOTE: This calculation extends a theoretical decay curve back to the beginning of the pulse or flash

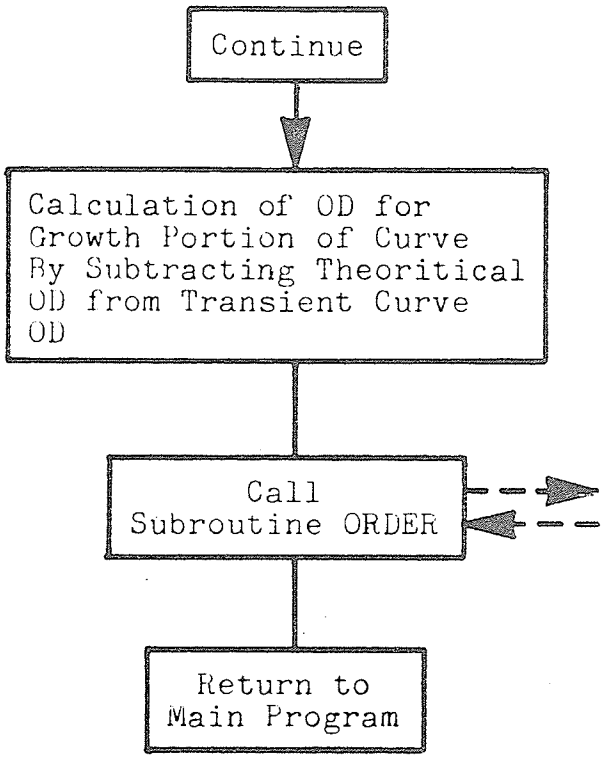
Continue
Calculation of OD for Growth Portion of Curve By Subtracting Theoritical OD from Transient Curve OD
Call Subroutine ORDER
Return to Main Program

Subprogram - "Data Analysis"

```
C - PROGRAM TO DETERMINE THE RATE CONSTANTS OF A SPECIES FROM CURVES
C - OBTAINED FROM A PULSE  RADIOLYSIS OR FLASH PHOTOLYSIS OSCILLOGRAM
C-
      DIMENSION X(1,200), Y(1,200), OD(1,200), EXP (15)
      DOUBLE PRECISION DC, X, Y, OD, SLOPE, SDEV, INTCP
      INTEGER CASE, N, J, K,D,IDAT,MTH,IPHOT,IWAVE
      REAL CONC, DLEV, DOSE
C-
C- DC- LIGHT LEVEL AND THE TYPE OF CURVE READ IN HERE
C- IF CASE  = 0, THIS SIGNIFIES A CURVE WHICH HAS BOTH A GROWTH AND DECAY
C-     SHOWN
C- IF CASE = 1 , THEN THE DATA IS JUST A SIMPLE DECAY
C-
      READ 1000,FNAME
 1000 FORMAT (A5)
      CALL IFILE (8,FNAME)
      READ (5,109) EXP
  109 FORMAT (15A5)
    5 WRITE (6,103)
  103 FORMAT (1H1, 15X,35HRATE CONSTANT FOR TRANSIENT SPECIES,/,
     116X,35H**********************************,// )
      WRITE ( 6,110) EXP
  110 FORMAT (15X, 15A5,///)
      READ(8,100) IDAT,MTH,IYR,IPHOT,IWAVE,CONC,DLEV,CASE, DOSE, NUM
  100 FORMAT(3I2,2I3,E10.4,F6.1,I1,F5.3,I3)
      WRITE(6,106)IDAT,MTH,IYR,IPHOT,IWAVE,CONC, DOSE
  106 FORMAT (30X33HTHE DATE OF THE EXPERIMENT WAS   I7,1H/,I2,1H/,I2,/
     1,30X20HTHE PHOTO NUMBER IS ,16XI5,/,
     230X17HTHE WAVELENGTH IS 19XI5,/,
     3 30X36HTHE CONCENTRATION OF THE SOLUTION IS E10.2,/,
     430X30HTHE MONITOR READING (VOLTS) IS 8XF5.3,///)
      IF(CASE.EQ.1) WRITE(6,104)
  104 FORMAT (20X35HREACTION CONSISTS OF A SIMPLE DECAY,/,
     120X,35H**********************************,///)
      IF(CASE.NE.1) WRITE (6,105)
  105 FORMAT (20X64HREACTION CONSISTS OF A GROWTH PORTION FOLLOWED BY A
     1SIMPLE DECAY,/,
     220X,64H****************************************************************
     3******,///)
      N = 0
      J = 0
      D = 0
      DC = 0.00D 00
      DC = DLEV
      SLOPE =0.0D 00
      SDEV = 0.0D 00
      INTCP = 0.0D 00
    1 N = N + 1
      X(1,N) = 0.000D 00
      Y(1,N) = 0.000D 00
      READ (8,101) X(1,N), Y(1,N)
  101 FORMAT (D15.4,D14.4)
```

```
      IF(X(1,N),NE,0.D0) GO TO 1
      IF (Y(1,N),NE,0,0D0) GO TO 1
      N = N - 1
      DO 500 K = 1, N
      J = J + 1
      X(1,J) = X(1,K)
      IF (DC,EQ,0,D0) GO TO 2
      OD(1,J) =  DLOG10(DC/(DC-Y(1,K)))
      GO TO 500
    2 OD (1,J) = Y(1,K)
  500 CONTINUE
      IF (CASE,EQ,1) GO TO 3
      CALL GROWTH (X,OD,J)
      GO TO 4
    3 K = 1
      CALL ORDER (X,OD,J,K, SLOPE, SDEV, INTCP, D)
    4 READ (8,107) M
  107 FORMAT (I10)
      IF (M,EQ,1) GO TO 5
      WRITE (6,102)
  102 FORMAT (1H1,19HEND OF CALCULATIONS)
      STOP
      END
```

```
      SUBROUTINE GROWTH (X,Y,L)
      DOUBLE PRECISION M, M1, M2, C, DIF, SLOPE, SDEV, INTCP,BEXP,X , Y
      DIMENSION X(1,200),Y(1,200)  ,C(1,200),DIF(1,200)
      INTEGER K,J,D,L
      WRITE (6,100)
  100 FORMAT (25X21HSIMPLE DECAY CONSTANT,///)
      K = 1
      D= 0
      SLOPE = 0.0D 00
      INTCP = 0.0D 00
      SDEV = 0.0D 00
      DO 500 J = 1 , L
      M = (Y(1,J+4)-Y(1,J))/(X(1,J+4)-X(1,J))
      IF (M.LT.0.0) GO TO 1
  500 CONTINUE
    1 J = J + 1
      M1 =       (Y(1,J+7)-Y(1,J))/(X(1,J+7)-X(1,J))
      M2 =       (Y(1,J+9)-Y(1,J+2))/(X(1,J+9)-X(1,J+2))
      IF (M1.GT.M2) GO TO 1
      CALL ORDER (X, Y, L, J, SLOPE, SDEV, INTCP, D)
      WRITE (6,101)
  101 FORMAT (25X 15HGROWTH CONSTANT, ///)
      IF (D.EQ.2) GO TO 2
      DO 502 K= 1,J
      C(1,K) = INTCP*DEXP(-SLOPE*X(1,K))
      BEXP = DEXP(-SLOPE*X(1,K))
  502 DIF(1,K) = C(1,K) - Y(1,K)
      GO TO 3
    2 DO 503 K = 1 , J
      C(1,K) = INTCP/(1.0 + INTCP*SLOPE*X(1,K))
  503 DIF(1,K) = C(1,K) - Y(1,K)
    3 J = K
      J = 1
      CALL ORDER ( X, DIF, K, J, SLOPE, SDEV, INTCP, D)
      RETURN
      END
```

```
      SUBROUTINE ORDER (X,Y,L,K,SLOPE,STDM,INTCP,Q)
C- L= TOTAL NO. OF COMBINATIONS OF X AND Y
C- K = IS THE ARRAY NO. WHICH BEGINS THE EXEXCUTION OF X AND Y COMB.
C- SLOPE = IS THE SLOPE OF THE LINE = CHANGES DURING EXECUTION OF SUBR.
C- SDEV = IS THE STANDARD DEVIATION OF THE Y AXIS
C- INTCP = IS THE INTERCEPT OF THE LEAST SQUARES FIT
C- Q = SIGNIFIES WHETHER THE LEAST SQUARES FIT IS FIRST OR SECOND ORDER
      DIMENSION W(1,200),X(1,200),Y(1,200), SLOPE1(4), S(2)
      DOUBLE PRECISION W,Y,X,SUMY,SUMX,SUMXY,SUMY2,SUMX2,SLOPE1,BASE,
     1INTCP,STDM,AO,SLOPE,HLIF,SUMY1,S,R
      INTEGER Q,P,J,M,N,F,K,G,L
      Q = 0
      DO 200 P = 1,2
      DO 300 J = K,L
      IF (P.EQ.1) GO TO 8
      W(1,J) = 1.00D 00/Y(1,J)
      GO TO 300
    8 W(1,J) = DLOG(Y(1,J))
  300 CONTINUE
      DO 400 M = 1, 2
      N = 0
      F = K
      G = K + 10
      IF (M.EQ.2) GO TO 7
      GO TO 6
    7 F = L - 10
      G = L
    6 SUMY = 0.00D 00
      SUMX = 0.00D 00
      SUMXY = 0.00D 00
      SUMY2 = 0.00D 00
      SUMX2 = 0.00D 00
      Q = Q + 1
      DO 500 J = F, G
      N = N + 1
      SUMY = SUMY + W(1,J)
      SUMX = SUMX + X(1,J)
      SUMX2 = SUMX2 + X(1,J)**2
      SUMXY = SUMXY + W(1,J)*X(1,J)
  500 SUMY2 = SUMY2 + W(1,J)**2
      BASE  = N * SUMX2 - SUMX**2
  400 SLOPE1(Q)= (N*SUMXY-SUMX*SUMY)/BASE
  200 CONTINUE
      S(1) = SLOPE1(1)/SLOPE1(2)
      IF(S(1).GT.1.0D 00) S(1) = SLOPE1(2)/SLOPE1(1)
      S(2) = SLOPE1(3)/SLOPE1(4)
      IF(S(2).GT.1.0D 00) S(2)=SLOPE1(4)/SLOPE1(3)
      Q = 2
      IF(S(1).GT.S(2)) GO TO 17
      GO TO 10
   17 Q=2
```

```
  10 N = 0
     IF(Q.EQ.1) GO TO 13
     WRITE (6,103)
     GO TO 14
  13 WRITE (6,100)
 100 FORMAT(25X,20HFIRST ORDER REACTION,////)
 103 FORMAT ( 25X,22HSECOND ORDER REACTION, ////)
  14 SUMY = 0.00D 00
     SUMX = 0.00D 00
     SUMXY = 0.00D 00
     SUMY2 = 0.00D 00
     SUMX2 = 0.00D 00
     DO 800 J = K,L
     N = N + 1
     IF (Q.EQ.1) GO TO 11
     W(1,J) =  1.00D 00/Y(1,J)
     GO TO 12
  11 W(1,J) = DLOG(Y(1,J))
  12 SUMX = SUMX + X(1,J)
     SUMY = SUMY + W(1,J)
     SUMX2 = SUMX2 + X(1,J)**2
     SUMY2 = SUMY2 + W(1,J)**2
 800 SUMXY = SUMXY + W(1,J)*X(1,J)
     BASE  = N * SUMX2 - SUMX**2
     SLOPE     = (N*SUMXY-SUMX*SUMY)/BASE
     INTCP  = (SUMX2*SUMY - SUMX*SUMXY)/BASE
     SUMY1 = 0.00D 00
     DO 900 J = K, L
 900 SUMY1 = SUMY1 +(W(1,J)-(SLOPE*X(1,J)+INTCP))**2
     STDM = DSQRT((SUMY2-INTCP*SUMY-SLOPE*SUMXY)/N)
     R=(N*SUMXY-(SUMX*SUMY))/DSQRT((N*SUMX2-SUMX**2)*(N*SUMY2-SUMY**2))
     IF (R.LT.0.0D 0) R=-R
     IF (Q.EQ.1) GO TO 15
     AO = 1.00D 00/INTCP
     GO TO 16
  15 AO = DEXP(INTCP)
     SLOPE = -SLOPE
     HLIF = 0.693D 00/SLOPE
  16 WRITE (6,101) SLOPE, AO, STDM, R
 101 FORMAT(30X,20HTHE REACTION RATE IS,D28.5,/,30X,16HTHE INTERCEPT IS
    1,D32.5,/,30X,33HTHE STD. DEVIATION OF THE RATE IS ,D15.5,/,
    2 30X25HTHE CORRELATION FACTOR IS 8XD15.5)
     IF (Q.EQ.1) WRITE (6,102) HLIF
 102 FORMAT (30X,31HTHE HALF LIFE OF THE SPECIES IS, D17.5,/////)
     INTCP = AO
      CALL PRTPLT (X,W,1,L,200)
     RETURN
     END
```